A

PROJECT REPORT

ON

APPLICATION OF ELECTROLYTIC IRON POWDER FOR DEVELOPMENT OF DIAMOND CUTTING TOOLS

SUBMITTED BY

UTKAR VIPUL VISHWANATH

M.Tech (Process Metallurgy)

(Roll No.-M0932R12/ MIS No.120927002)

UNDER THE GUIDANCE OF

Dr. N. B. DHOKEY

DEPARTMENT OF METALLURGICAL ENGINEERING

AND MATERIAL SCIENCE

COLLEGE OF ENGINEERING

PUNE-411005

(2010-2011)

ACKNOWLEDGEMENT

This acknowledgement is not a mere formality, but it is penned to express my sincere gratitude towards everyone who has contributed towards making my project work a memorable experience.

I express my sincere thanks to our Head of Department, Prof. Dr. M.J. Rathod for giving me an opportunity to carry out this project work. I have a deep sense of gratitude, appreciation and indebtedness to my guide, Dr. Prof. N.B.Dhokey for his keen interest, proper guidance, constant encouragement and substitution support throughout the project work. Because of him only this project work is carrying technical importance.

I am also thankful to Mr. Praksah Dhoka (M.D, IMP India Pvt. Ltd.Pune) for sponsoring this project work. I express my sincere gratitude towards to Mr. Ashok Gosavi (IMP India Pvt.Ltd.Pune) for providing facility for conducting industrial trialsI would like to thank to management and staff of IMP India Pvt.Ltd., Pune for providing all the necessary supports and information regarding this project.

I am thankful to Mr. Kalagutakar, Super Cut Tools, Mumbai for allowing me to use their setup for final prototyping of diamond Cutting tools.

It is my duty to express my thanks to Dept.of Physics, University of Pune and VNIT, Nagpur for providing SEM facility and IIT. Bombay, Mumbai for carrying out initial characterization of powders.

I am very much thankful to all the staff of Dept of Metallurgy and Material science, Govt. College of Engg. Pune. who helped me directly or indirectly a lot for completion of my project work. Along with them it was a memorable experience to work with my colleague, Janhvi Dandawate, Snehal Jadhav, Kedarnath Rane and all my friends of COEP.

Vipul V.Utkar

Abstract

Diamond cutting tools are widely used in Stone/marble cutting industries. These tools are finding promising market for its manufacturing and indigenization in Indian industry using available resources. The present work analyses two cutting tools viz. 1) Diamond cutting wheel and 2) Gang Saw bead for chemical analysis, optical, SEM-EDX, wear resistance, bulk hardness, etc. Based on the findings of these diamond cutting tools, a laboratory simulation was done using imported powders normally used for manufacturing these diamond cutting tools were investigated for particle size distribution using Laser particle analyzer and subsequently the imported powders were compacted with H/D less than 1 at 550MPA and sintered at 870°C for 30 minutes in hydrogen controlled atmosphere. These sintered compacts were measured for sintered density, microstructures analysis, SEM-EDX, etc. and wear loss study using Pin-on-Disc machine on sintered alumina counterface materials. After finding optimum composition the premix was taken to industry and prototyping of the tool is done. The final prototypes were also subjected to testing and characterization and the results were compared with existing tools. Though using premixing methods, major used of electrolytic Fe powder and reducing Co amount the fabricated tools show better properties than existing one.

CHAPTER-1

INTRODUCTION

1.1 Background:

Diamond is the hardest material known to man till now. In spite of hardness, diamond also possesses some unique properties like highest conductivity, almost inert to chemical attack, very low thermal expansion and most important diamond has cutting edges by which it can cut the other material. These properties of diamond make it as a very important cutting tool in industry as well as in other cutting applications. Much faster development in this field has been seen over last 50 years and more, which attributed to the invention of synthetic diamonds. Modern developed diamond tools are used in stone cutting, construction, road repair, wood working, production of various parts made of glass, ceramics, metals, plastic, etc.

1.2 Current challenges in diamond cutting tools:

Diamond cutting tools (DCT) are mainly prepared by two ways. First one is by impregnating diamond particles in prealloyed powder prepared by co-precipitation method and second one by premixing of metal powders. Today's scenario, either mainly imported readymade prealloyed powders or premix powders of alloying elements are used. There is always a difference of opinion about the quality of resultant diamond cutting tools. Chiefly Co, Cu and Fe are the major metal powders used for preparing DCT, out of which Co is expensive which decides the cost of tool. Another important issue in the manufacturing DCT is the formulation of chemical composition which remains the propriety of the manufacturer. In order to reduce the dependency on the imported powders, manufacturer of diamond cutting tools are trying hard to use indigenous materials as far as possible. Hence a more concentrated efforts are needed to develop the materials both from technical point of view as a well as from commercial viability point of view.

1.3 Approach of the present work and Report Organization:

Present approach for this project work can be stated as per following manner,

Chapter-2 (Literature Review) gives the idea about fabrication of diamond impregnated cutting tool and information regarding prior work.

Chapter-3 (Experimental Work) briefly explains the methodology in selection of material, procedure adopted for analysis of existing DCTs, metallographic and mechanical property characterization and about sintering parameters selection.

Chapter-4 (Metallurgical Investigation Of Diamond Cutting Tools and Pre-Alloyed Powders) This chapter deals with analysis of two types of existing DCTs and two types of pre-alloyed powders from various tests like wear test, hardness test and microstructure analysis and chemical tests.

Chapter-5 (Results and Discussions) throws light on the outcome of the present work regarding effectiveness of electrolytic Fe powder in development of premix for DCTs manufacturing. It also stresses about optimizing Co% in those premixes.

Chapter- 7 (F**uture Scope**) deals with the future line of action for the development of DCTs particularly regarding their modeling and wear resistance improvement.

CHAPTER - 2
LITERATURE REVIEW

Powder metallurgy is the most efficient way to manufacture diamond tools. Synthetic diamonds are impregnated in the matrix of Copper, Cobalt and Iron. The two basic functions of any metal matrix are to hold diamond particles and to erode at a rate compatible with the diamond loss. The cobalt metal used in the matrix perform very basic function of holding the diamond pieces due to unique combination of high yield strength and toughness, this is hardly attain by any other metal. The scientists are taking many efforts to reduce the cobalt percentage in this matrix because of its high cost. A brief literature review on fabrication of diamond impregnated cutting tool is presented.

2.1 About Powder metallurgy:

As stated above, powder metallurgy (P/M) is the most efficient technique to produce cutting tools. P/M process has the ability to fabricate high quality, complex parts to close tolerances in an economical manner. P/M takes a metal powder with a specific attributes of size, shape, and packing then converts it into a string precise, high performance shape. Also P/M is a flexible manufacturing process capable of delivering new range of materials and properties. Recently all metal-bonded tool components involve many powder metallurgy operations.

Basic steps include,

I. Powder preparation.
II. Compaction
III. Sintering,

Following figure illustrates the P/M process for diamond tool preparation in detail,

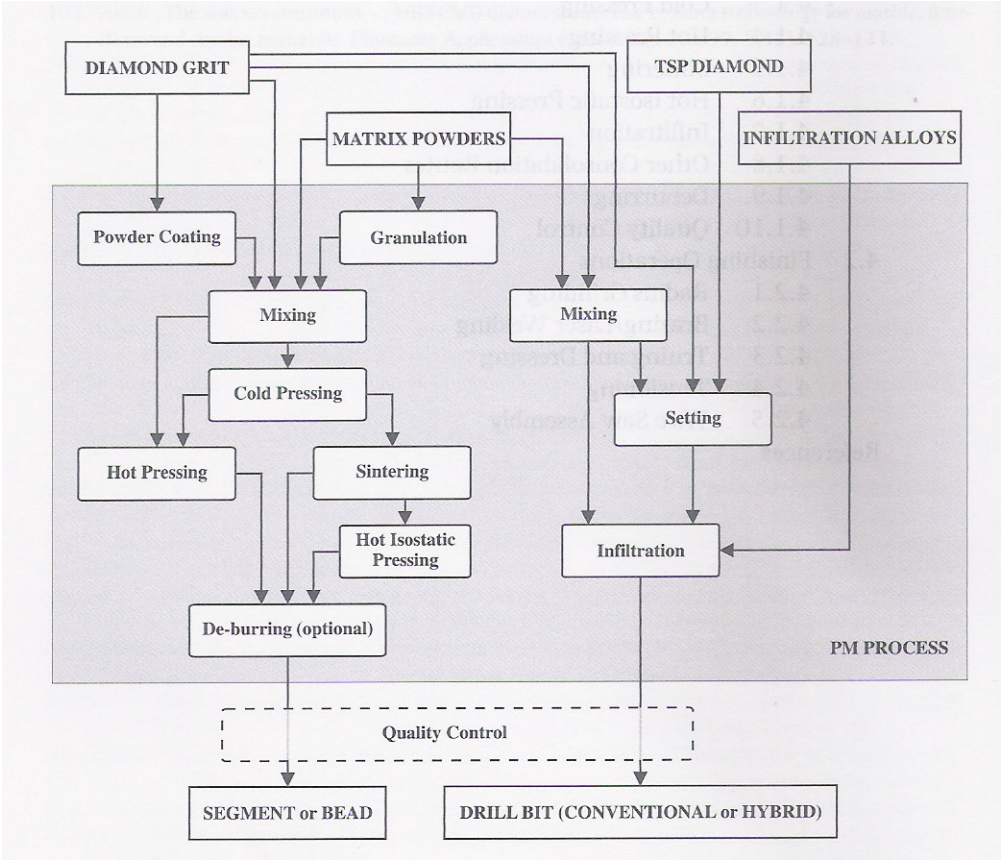

Fig: 2.1 P/M diamond tool production process [1]

Powder preparation:

Basic step in P/M process starts with powder preparation, in which powder of selected materials (in this case mainly Fe, Cu, and Co) is mixed in a proper manner with the help of mixer also some time called as blender. Binding agents and lubricants are also added while mixing. Mixing is carried out in different types of blenders as conical, cylindrical etc. complete process parameters are selected according to shape and size distribution of the final product.

Matrix-diamond Mixture preparation:

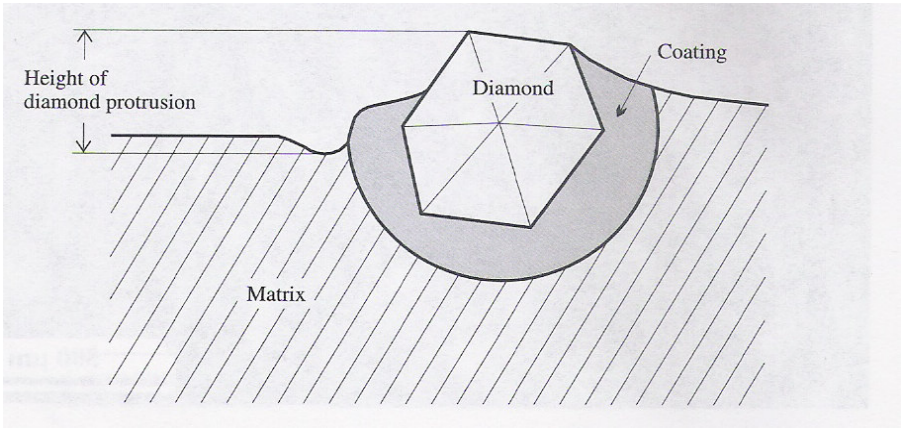

Fig 2.2: Positive effect of wear resistant coating on diamond particle protrusion [1]

With respect to diamond tool preparation diamond particles are usually coated prior to mixing with matrix powder. This is done to avoid the premature wear of the tool due to non uniform distribution of the matrix powder and diamond particles. Also life of the die increases if we used coated diamond particles as it helps in efficient ejection. Diamonds are coated by making the homogeneous slurry of the matrix powder with binder dissolved in volatile organic solvent. This slurry is then spread onto a bed of warm air-fluidized diamond grits.

Compaction:

Conventional compaction process consists of compacting the powder inside die between upper and lower punches. It is also called as uniaxial compaction as in this; pressure is applied along one axis. Following figures explain the idea about compaction process.

Now a day's many modern techniques are used by industry like hot compaction, isostatic compaction which further helps in densification of the final product. Normally in tool preparation compacting pressure varies from 400 MPa to 600 MPa. After compaction, the compact must be removed from the die, the force required for ejecting

the compact is names as ejection force. This force is considered while selecting the lubricant. The sample or compact obtained in this process in defined as green sample.

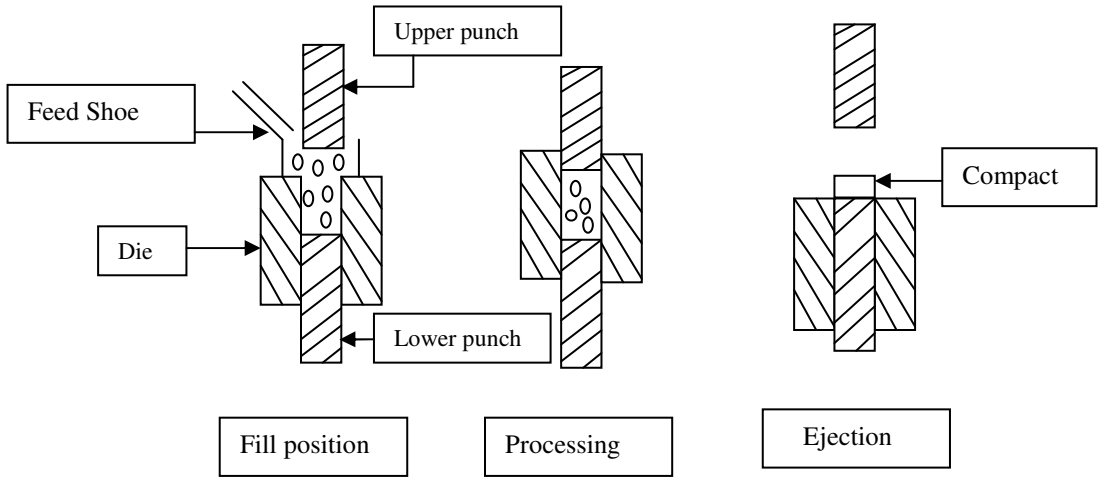

Fig 2.3 Compaction process [2]

Sintering:

Sintering is final step in P/M process, in which the green sample is heated in furnace at its sintering temperature in reducing atmosphere of hydrogen and nitrogen. Sintering temperature is the temperature at which binding between the powder particles or grains occurs and it gets sintered. This temperature is different for different metals. To avoid oxidation of metal powder at high temperature reducing atmosphere is provided, in which firstly flushing is carried out by nitrogen gas and then hydrogen gas is injected in the furnace. The ratio of hydrogen to nitrogen is maintained as 10:90 and while finishing the process again flushing is performed. The hydrogen which comes out from the furnace is burnt to avoid the explosion.

Sintering phase can divided into two main types as,

i. *solid state sintering-*

Solid state sintering can be defined as, sintering of the powder mixtures without solid solubility exclude interdiffusion between two particles. Homogenization depends upon particle size distribution, sintering time, sintering temperature. At high temperature, sintering rate is faster because of increase in number of active atoms. Most composite

systems are difficult to manipulate during sintering. Also, if two insoluble powders are sintered, they result in typical degraded sintering. To enhance solid state sintering different techniques are using such as by phase stabilization activated sintering.

It is observed that stabilization of the BCC phase provide more rapid sintering, hence in case iron materials, elements like molybdenum, phosphorus, silicon stabilize ferrite above its polymorphic transformation temperature. While austenitic stainless steels can be stabilized by using nickel.

Activated sintering refers to several techniques which lower the activation energy, allowing for a lower sintering temperature, short sintering time and better properties. By using techniques like chemical additions, application of external electric field. Activator should be either metal or compound which forms a low melting temperature phase during sintering and the activator must have a large solubility for the base metal.

ii. liquid phase sintering-

In liquid phase sintering once the liquid forms, it will flow to wet the powder particles. Figure 2.4 explains the liquid phase sintering mechanism. Reduction occurs in dimensions of the green sample during sintering process due to densification takes place. This change in dimension should be considered while designing the final product dimensions. In case of diamond tool manufacturing process sintering temperature varies from 850 to 950 ^{0}C and soaking time as 30 minutes.

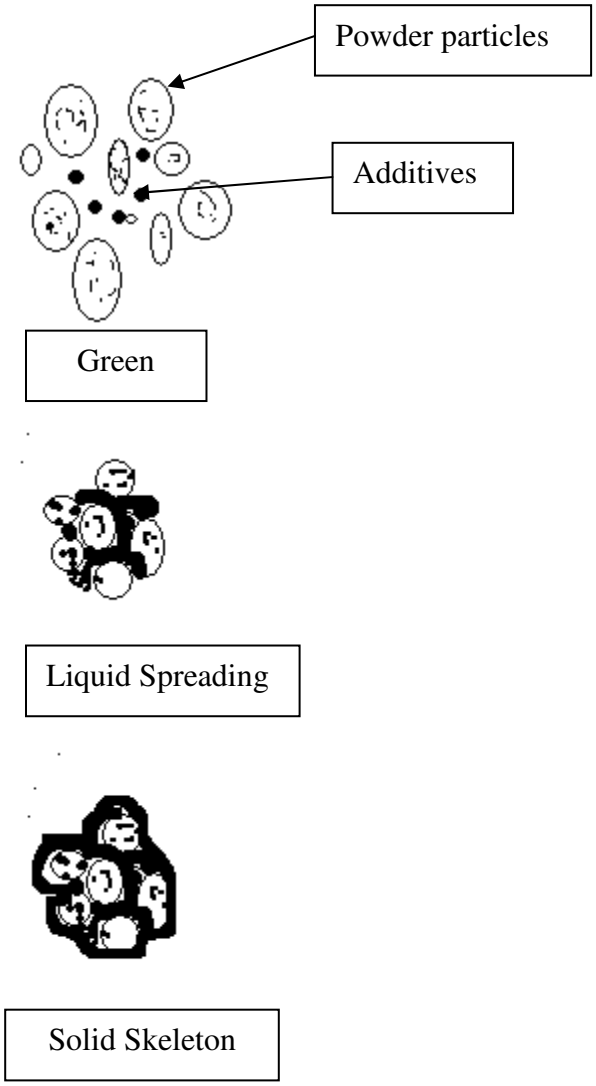

Fig.2.4: Liquid phase sintering process [2]

2.2 Reinforcement types in cutting tools:

Reinforcement should be harder than the material which has to be cut. Generally Tungsten carbide (WC), Silicon carbide (SiC), titanium di-boroid (TiB2), and off course diamond are the hard materials used as a reinforcement in cutting tool.

2.3 Selection of reinforcement in metal matrix:

In case of diamond cutting tools, diamond particles are impregnated into the metal matrix. It decides wear performance of the tool. Diamond performs the main function,

i. Prevent the matrix from direct rubbing against the processed material

ii. Help in direct blockage of abrasion grooves

Diamond particle loss or protruded from the surface, the immediately matrix tail is exposed to the wear and in very short time tool will worn out.

Optimum diamond concentration in the metal matrix is the complex function depends on its size, type, tool operating parameters, work piece properties and machine conditions. It is important that diamond crystals are uniformly distributed throughout the matrix. The property by which diamond is the best cutter due to its extreme sharpness with cutting edges which is not found in other. Thus diamond particle can be used for precision cutting also.

2.4 Morphology of diamond:

In case of synthetic diamonds morphology of these diamonds can be created by the synthesis process conditions. It can vary from cube to octahedral named as cubo-octrahedral. Figure 2.5 shows the cubo-octahedral morphology of the diamond particle .Morphology index is assigned to diamond crystals. The diamond shape affects the cutting property of the tool. Diamonds which have regular cubo-octahedral shape are stronger than irregular diamond crystals with less defined cutting edges and rough faces. But less crystalline grits are freer cutting in application. Weaker diamond crystals with good retention properties are required in the frame sawing.

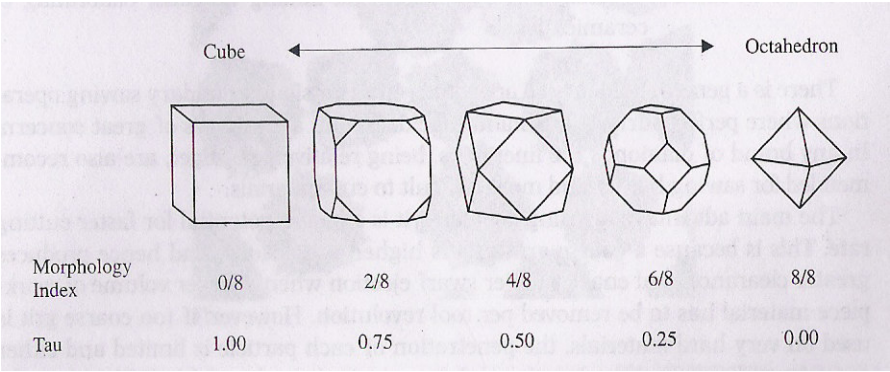

Fig.2.5: Dynamic representation and numeric codes of various synthetic diamond morphology

2.5 Properties of diamond:

Some unique properties of diamond can be enlisted as,

i. Allotropic form of carbon
ii. Hardest mineral
iii. Highest Thermal conductivity at room temperature.
iv. Low coefficient of friction
v. Low coefficient of thermal expansion
vi. Almost inert to all types of chemical attack.

Synthetic vs natural diamond

Besides this as explain above diamond are classified as synthetic and natural diamond, Natural diamonds which are made by crushing mined diamond boart, are free from metallic inclusion hence show excellent thermal stability. They can retain their original mechanical strength even up to 1400^0C whereas synthetic diamonds begin to lose their strength beyond 800^0C. The main advantage of using synthetic diamond is that it can be designed and manufactured to any specific application requirements. Two main grades of synthetic diamonds are available in the market as cobalt grade and nickel grade. Cobalt grade is mostly used for tool applications while nickel grade is used for decorative purposes as it is transparent.

Effect of sintering on diamond

Degradation of diamond can occur during sintering. It depends on the sintering temperature, chemical composition of the metal matrix, metal particle size and its distribution. In diamond impregnated tools, diamond degradation generally starts at 800 ^{0}C. Graphitization is the primary cause of this. Generally finer the grit, higher the temperature, longer the hot pressing time, the greater the degree of graphitization. Cobalt, tungsten, nickel, and iron are known as carbide formers and when these metals are used as matrixes the diamond crystals integrity is affected by surface graphitization during

sintering. But sintering with copper, bronze material does not affect the integrity because of its poor chemical affinity.

2.6 Influence of Cobalt, copper and iron:

Selecting Co as one of the basic metal as it performs following functions,

i. Wear resistance
ii. Diamond retention capacity

A soft matrix wears faster than diamond, which results in possibility of diamond becoming detached. Cobalt helps to provide hardness and wear resistant which wears the tool ideally as fresh diamond cutting points are exposed progressively after the initial diamond particles are blunted.

Diamond tool performance is determined by the retention capacity. Diamond is bonded in the metal matrix powder through compression and then sintering. Cobalt is metal which help in retention of the diamond crystals. In other words, cobalt increases diamond particles holding capacity of the tool.

Iron along with cobalt and sometimes nickel if added help in formation of bonds and provides necessary strength to tool. Copper having low melting point serves as a binder in tool. It helps in holding the grains of other metal powder. Copper also helps to fill the gap between to particles or grains. It goes into the grain boundaries by which structure becomes more densify. Copper provides necessary softness and wear resistance to the segment. Equilibrium diagrams help to find out solubility and sintering temperature.

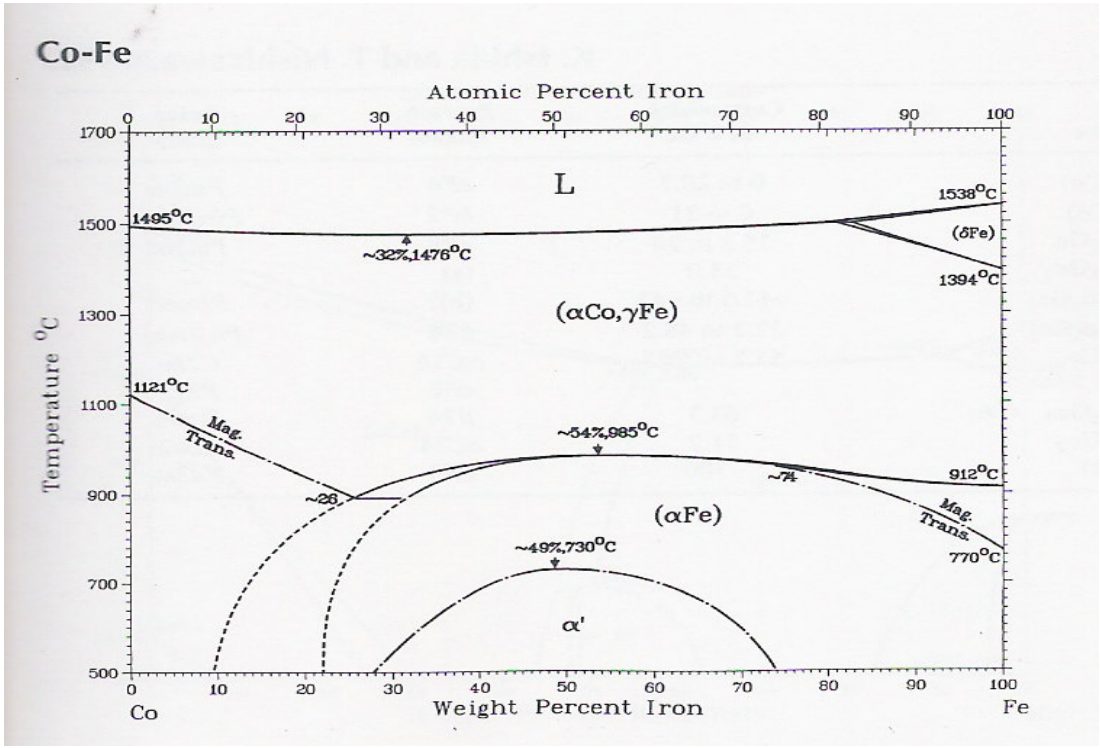

Fig; 2.6 Fe- Co equilibrium diagram

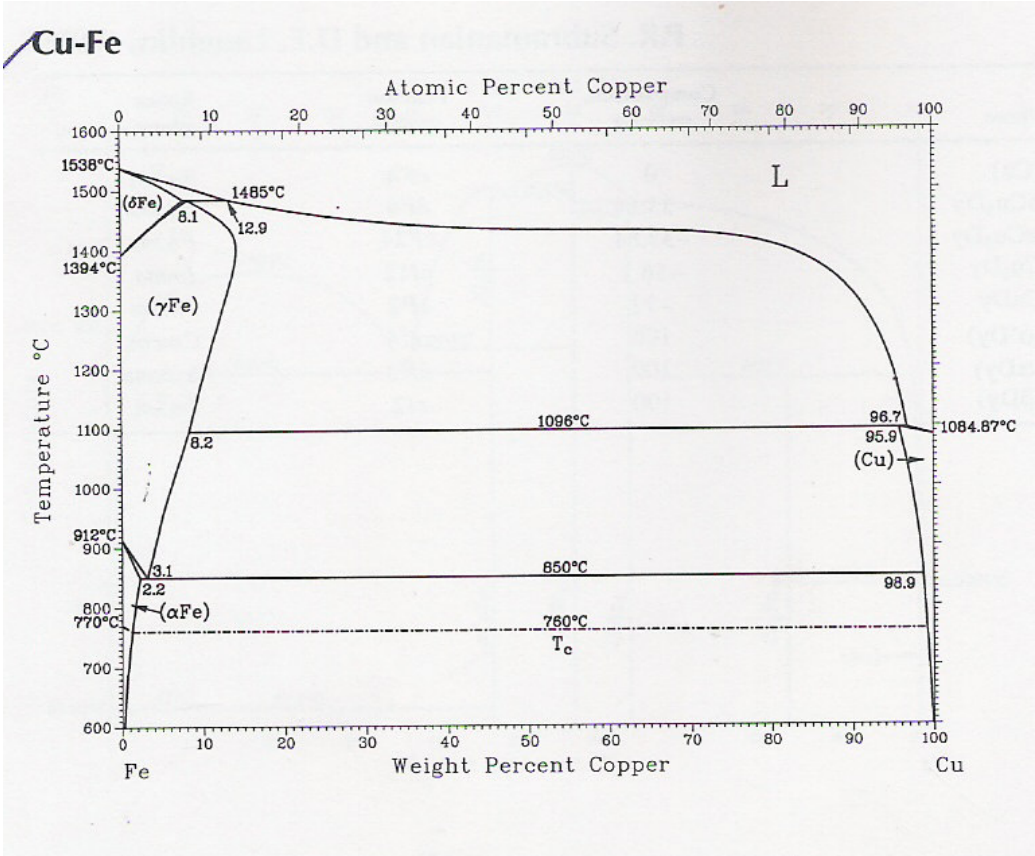

Fig.2.7: Cu-Fe equilibrium diagram

2.7 Prior work:

Steven W. Webb et.al. [4] described a method for evaluating retention and demonstration how coatings on diamond can improve retention and tool performance.

He has constructed a formula, which give idea about good diamond retention. According to him, crystal retention may be quantified as ratio

$$R = \frac{\text{(Contact area) x (Matrix compressive stress) x (Diamond–matrix friction)}}{\text{Contact force}}$$

If R > 1, the crystal has good retention with the bond matrix. Higher R can be achieved by with good bond exhibiting high compressive stress from sintering, as well as high level of friction and adhesion between the diamond and the matrix. The force and geometry of the bound crystal is shown in Fig 2.8.

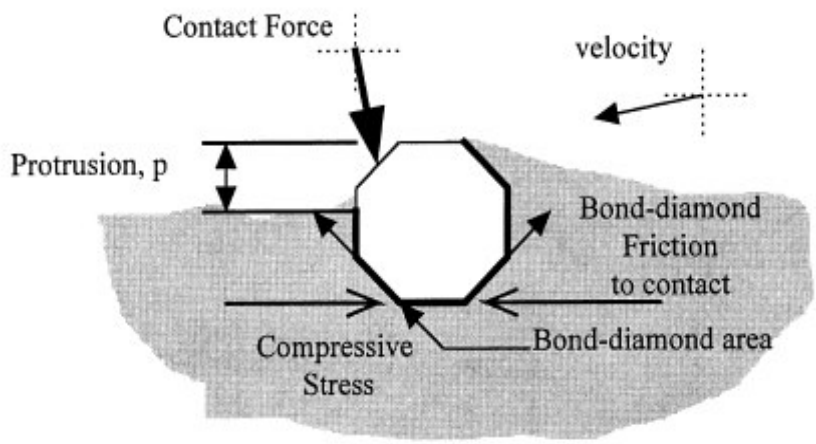

Fig 2.8: Forces on working diamond cutting point in a drill or saw blade; force, velocity relative to machine table

Coatings help to increase the compressive stress which results in good retention properties. Also diamond coating provide higher friction while cutting helps to increase cutting ability of the tool.

Sadi Karagoz et.al. [5]**:** studied the bonding structure present between the diamond particles and the metal matrix. According to them reaction starts between diamond particle surface and metal matrix. This indicates presence of chemical bonding in addition to mechanical bonding.

For this, various diamond compositions are used for micrographical study. Standard EDX format is taken as a reference as shown in figure 2.9. Tools manufactured by P/M process the bonding phase is made up of Co, Fe and Ni while Cu and Sn used as filling phase which melts during sintering. In standard sample, Cu and Sn are present in the ration of 90:10 as given in figure 2.9. Transverse rupture test is used to determine toughness of the tool. The SEM images of fractured parts are obtained to analyse the interfacial bonding of diamond with matrix as seen in Fig 2.10

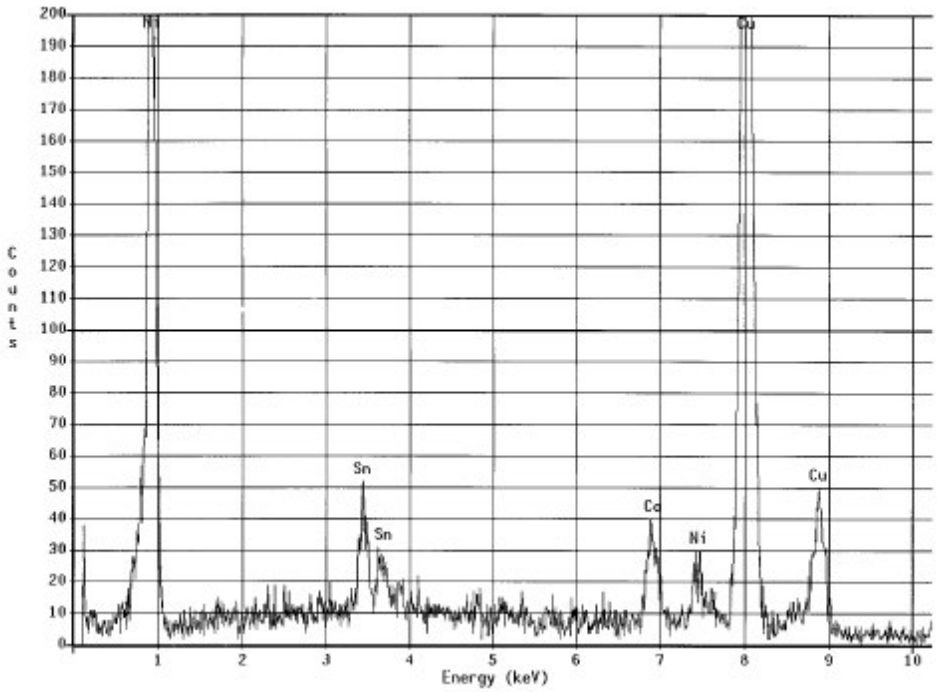

Fig. 2.9 EDX analysis of the matrix of the diamond-cutting tool which is used to cut natural stones.

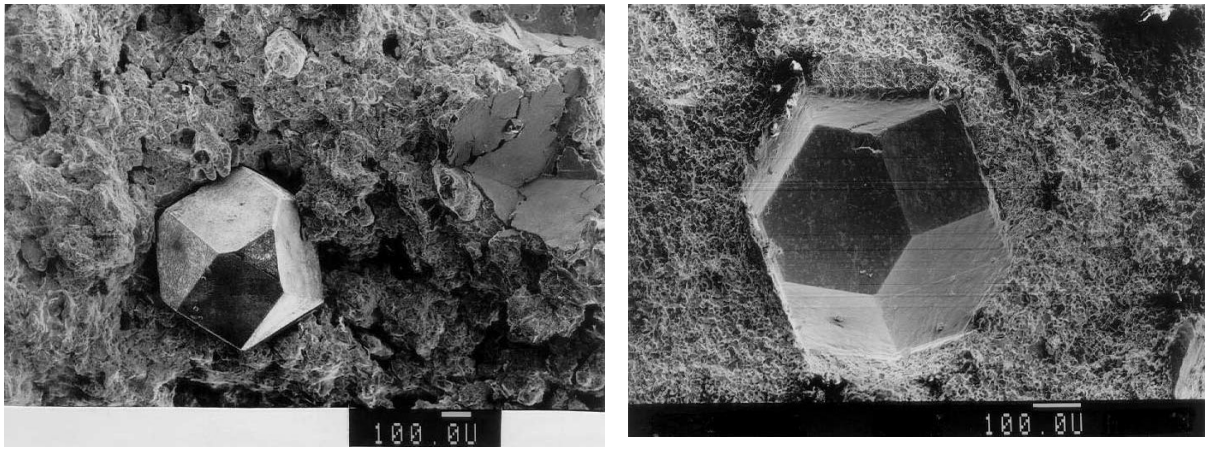

(a) (b)

Fig. 2.10: Comparison between (a) loose Bonding and (b) strong bonding

Weibull statistic (extreme value statistic) is applied to understand the defects present in tool. This method helps to give the information about active defects and their sizes. It is necessary to study this because initiation of the fracture stars with combination of the defects and stresses. As it can be seen that even diamonds are also counted as defects through their size, form and area distribution.

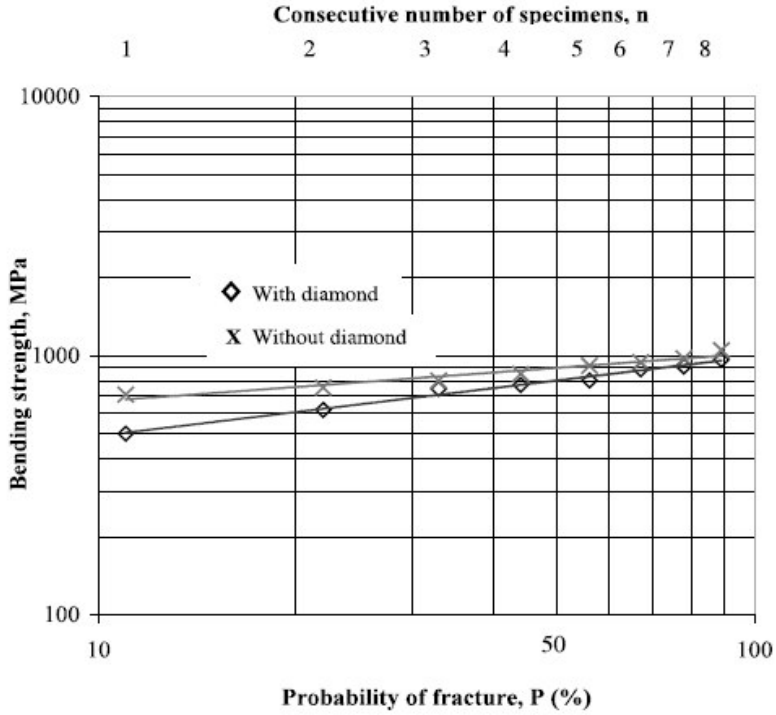

Fig 2.11: Three point bending test results interpreted in terms of Weibull statistics

Thus, it can be concluded that with the help of electron metallographycal techniques additional analysis or the failure analysis can be done. It also helps for characterization of the diamond tools. Besides this bond strength between diamond particles and matrix material is the most important for cutting tools. As this strength improved it will help to improve the cutting performance of the tool.

H.K. Tonshoff et.al. [6] gives the overview of the wear mechanism. This work also helps to predict suitable conditions required for efficient cutting. In case of wear, they divided wear into matrix wear on the one hand and diamond wear on the other hand. One mechanism that directly affects the diamond is the abrasive effect of the stone material, together with high mechanical and thermal loads of the process, which lead to wear of the grains. In the cutting process, sedimentary rock mainly fractures along its grain boundaries because of the low strength of its binding material.

Wear mechanisms affecting the diamond grains can be divided into four main forms:

1. Adhesion wear: the diamond sticks to the stone surface and particles are sheared off.
2. Friction wear: very hard grain particles of the rock scratch the diamond surface.
3. Wear by diffusion: chemical reactions between the work piece and the diamond surface lower the strength or the hardness.
4. Fracture of grains: fracture of the diamonds is caused by mechanical or thermal overload or by fatigue.

However, wear by adhesion and diffusion is not significant in the process of stones. Fracture of the diamonds and wear by friction are the major wear mechanism that causes a reduction of the grains. The wear form depends on the different loads during the cut. Fig 2.12 explains the wear mechanism. Under up-cutting conditions with a low cutting speed and a homogenous stone, the diamonds will be worn flat. High feed speeds under down-cutting conditions in processing a stone with hard zones will lead to fractured diamonds because of the shock load.

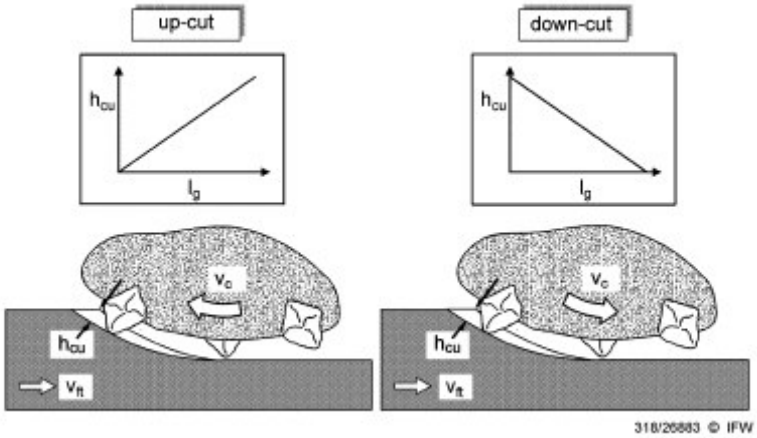

Fig.2.12: Single-grain chip thickness in up-and down-cutting **mode**.

The worn-flat grain is caused by high thermal load on the grain tip, while the mechanical impulse is not sufficient for fracture, i.e. the grain face area is too small or the cutting velocity too low. Fracture is caused by a mechanical impulse, requiring certain grain face area or cutting speed.

Matrix wear can be divided into

i. If the matrix wears too fast, the diamond capacity is not completely used before the diamond is pulled-out.

ii. If the matrix wears more slowly than the diamonds, the space between the cutting edges and the matrix is constantly reduced. The swarf (debris or waste resulting from metalworking operations) cannot be carried away properly, and the segment will continuously lose its ability to cut.

A characteristic feature of matrix wear is a crater in front of the single grains. Behind the grain, there is less erosion of the matrix; a bond tail is formed, so that the diamond is sustained against the process forces to remain in the bond.

C.Y. Wang et.al [7] discussed kinematic behavior of the frame sawing process.

According to them the sawing process of marble is unstable because the marble is inhomogeneous and the diamond segments are welded on the thin and long blades, which

move along a complicated path. In order to optimize the processing parameters and make good quality product with high productivity and low cost, both stone machining factory and diamond blades manufacturer need to understand the frame sawing better.

Kinematic analysis given by them is as follows,

Kinematical formula of frame sawing movement:

$$lc(t)= l_h/2\ (1-\cos 2\pi n_k t_s) \quad \text{----------(1)}$$

$$v_c(t) = \pi nklh\sin 2\pi n_k t_s \quad \text{----------(2)}$$

$$a_c(t)= 2l_h\pi^2 n^2_k \cos 2\pi n_k t_s \quad \text{----------(3)}$$

Where, the moving distance of blade lc, cutting speed (cutting forward or backward) Vc and a_c is the acceleration of blades can be described with the formulas as given above. Also, l_h is the stroke length, n_k is the round per minute (rpm) of crank and t_s (s) the cutting time.

Cutting path per diamond grit:

The blade moves forward by the movement of the craft to achieve the cutting motion while going down to achieve the feed motion. The paths of the contact points between the stone and diamond segments (or diamond grits), shown in fig 2.13 can be expressed by equation 4 and 5

$$x = l = l_h/2\ (1-\cos 2\pi n_k t_s) \quad \text{---------- (4)}$$

$$y = (V_f/60)\ ts \quad \text{----------(5)}$$

where ,V_f (mm/min) is the feed rate that the blade moves down.

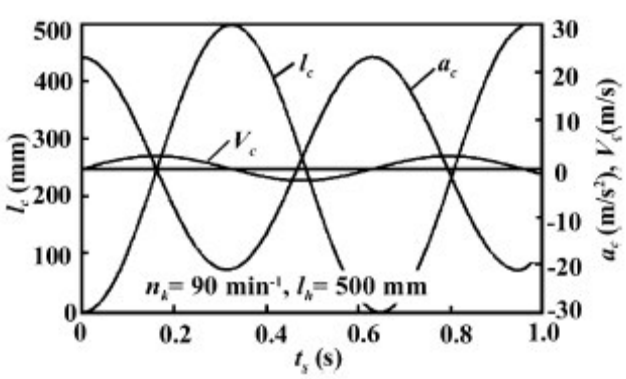

Fig.2.13: kinematic parameters in frame-sawing

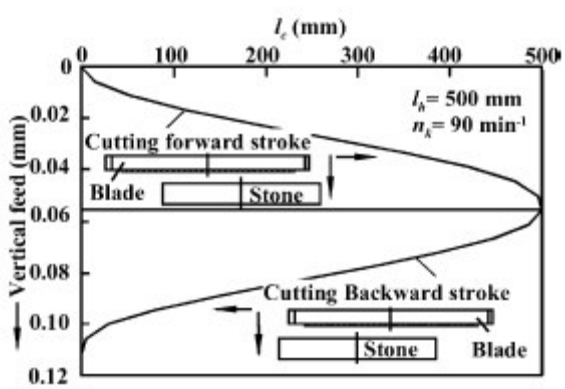

Moving path of a blade in a cutting stroke

From Eqs. (1)–(5) and Fig2.14 some basic features of the diamond grit in frame sawing can be summarized, as

i. At the beginning of forward cutting and backward cutting in a stroke cutting, the diamond grits that are in contact with the stone block are loaded by the impacting forces, where the depth of cut goes up about 2–6 μm in 33 ms.

ii. The number of effective cutting diamond grits and their effective depth of cut will depend on the segment position and protrusive height of the diamond grits on it.

iii. The depth of cut of the diamond grits increases with the increase in V_f and the decrease in n_k and l_h. The maximum depth of cut per grit a_{pmax} depends on both positions at the starting point and endpoint as they contact the stone in the half stroke cutting.

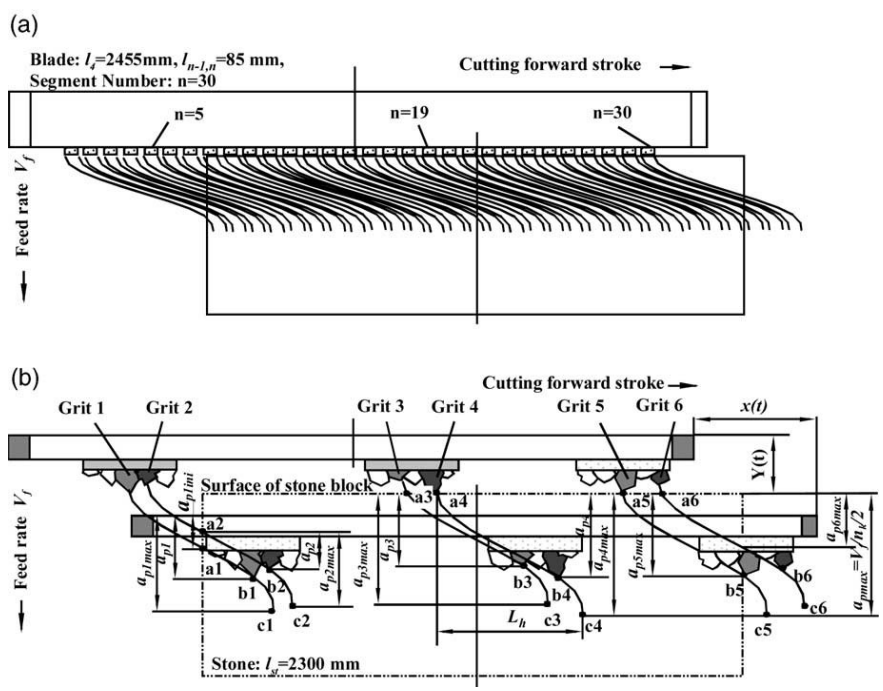

Fig.2.14: Cutting paths of segments and depth of cut of diamond grits in frame sawing (a) Cutting paths of segments (b) depth of cut of diamond grits.

Experiments performed on CNC milling machine. The cutting force Fc along the cutting direction and cutting force F_f vertical to the cutting direction are measured by a Kislter dynamometer (Type 5019). The single point cutting tools are sharp conical carbide tools made from the milling tool (conical angle 120°) and the single point dressing diamond

tool (conical angle is about 120°). They are used to simulate the cutting process of the diamond grit on a segment. Segment Type 3 is used for simulating the cutting process of segments. The segment size is 20 mm×4.8 mm×7 mm. The matrix of bond of the segment is Ni-based with hardness of HB30-240. Diamond MBS950 with mesh D302 (D301:D251=1:1) and concentration 22.72% is used. Based on the kinematical analysis in Section 2.2, the depth of cut in test is 5–45 μm; the feed rate is 500 mm/min and the indenting feed rate is 80 mm/min (vertical feed rate) for different cutting paths, such as normal cutting and indenting-cutting in different directions and positions. Two kinds of stones are tested with and without water. Thassos is a kind of white marble with fine grains made in Greece. Jura Gelb is a kind of cream-colored limestone mined in Germany. It has fine crystalline carbonate as well as much coarser crystallized shell relics and fossils of creatures. The groove topographies are observed by a microscope and recorded by the Video Image Capture System.

1) Cutting by a single point cutting tools:

As shown in Fig 2.15 the surface morphographics indicate that the chippings of lateral cracks develop with small depth of cut and the plastic deformation can be observed even with a larger depth of cut. The fracture of the stone causes craters on the side of the grooves and stops at the plastic deformation zone, located at the bottom of the grooves. The cutting forces increase almost linearly. As the figure 2.16 illustrates, dry cutting has larger cutting force than wet cutting. The cutting forces of the two kinds of stone are different when the depth of cut is small, but the difference between them becomes smaller as the depth of cut increases

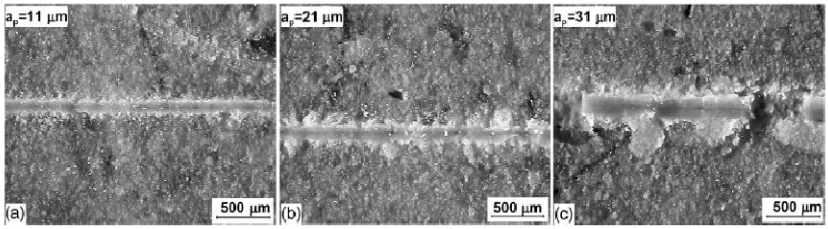

Fig 2.15: Jura Gelb cutting by a sharp conical carbide tool in wet cutting

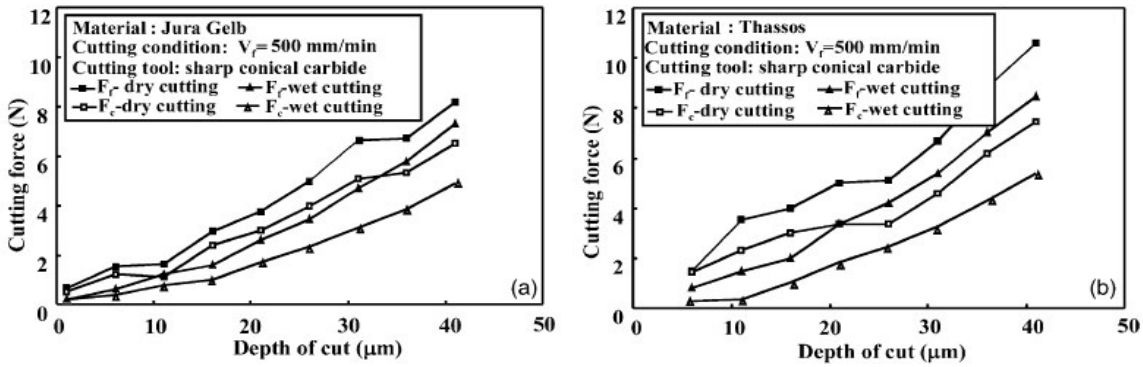

Fig. 2.16: Cutting forces by sharp conical carbide: (a) Jura conical carbide (b) Thassos cutting

.

2) Cutting by a single diamond segment:

.

Jura Gelb cut by a single segment is shown in Fig 2.17 (a1), (b1) and (c1) are the views of the total area cut by the segment at different depths. Each of the grooves cut by various diamond grits is marked with a serial number. The shallow groove No. 5 with plastic deformation can be found in figure (a2). When the depth of cut becomes larger, the depth of groove increases and the cracks develop to cause chipping as shown in figure (b2) and (c2). Groove No. 6 is found also within craters, cracks and residual plastic deformation in (a2). As the depth of cut reaches 10 μm, the residual crushed zone peels off and a rough surface of groove appears, as shown in (b2). The depth of groove will increase as shown in (c2). The interaction of the diamond grits in the cutting process can be observed clearly in (a3), (b3) and (c3). Three diamond grits cut at different positions with different depths in (a3). The grooves are labeled No. 1, No. 2 and No. 3. The crushed zones of groove No. 1 and No. 2 break off in (b3). The residual plastic deformation can be seen in groove No. 3 in (b3). Some of the cracks formed by three diamond grits have intercrossed each other. As the depth of cut reaches 15 μm, the intercrossing cracks cause the breakage of stone surface and then three grooves join into a broader groove in (c3). As the cutting process continues, the grooves form again for each of the diamond grits at the bottom of the wider groove due to the various protrusions of each of diamond grits of the segment.

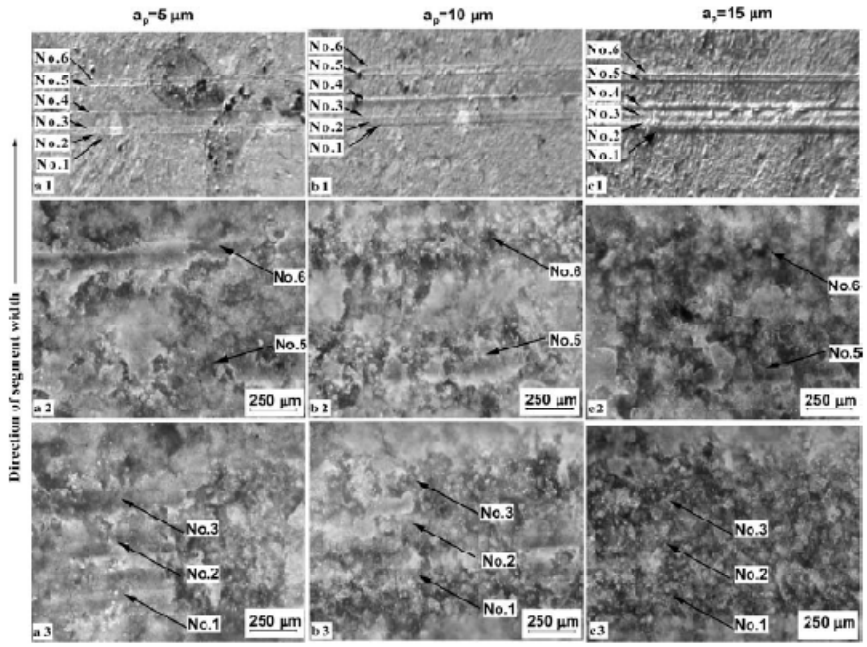

Fig. 2.17 Cutting of a Jura Gelb by a single diamond segment in wet cutting

Also it has been discovered that effective cutting diamond grits of the segment tested increases with increasing depth of cut.

Cutting mechanisms:

1) Single point cutting tool-

In case of single point cutting tool as shown in figure2.18, dressing diamond tool functioned both as blunt indenter and sharp indenter.

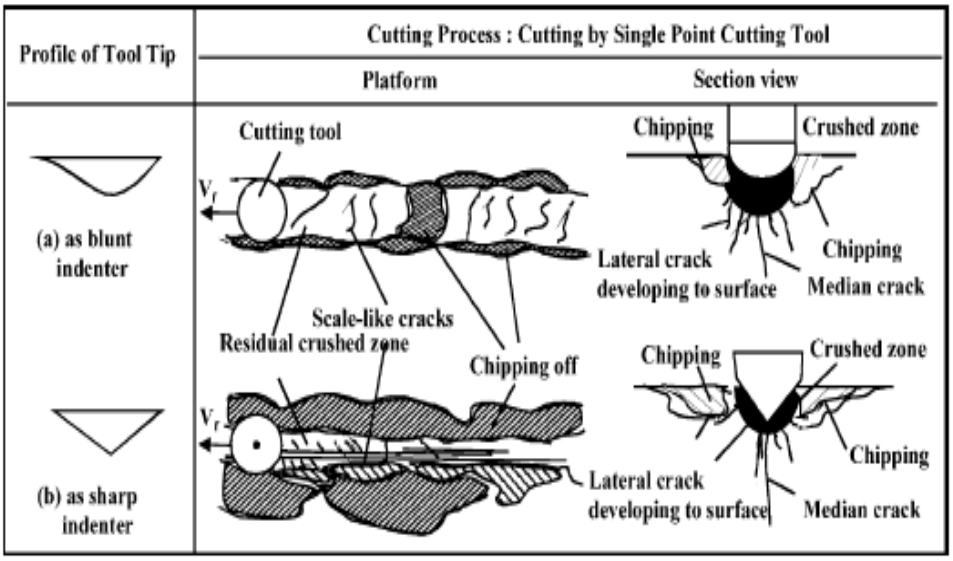

Fig 2.18: Cutting process of marble by single point cutting tool

2) Diamond segments-

The cutting process of the segment can be described as the cutting of a multi-point diamond tool with different depths of cut, as shown in Fig. 2.19. The development of cracks and the intercross of cracks due to the indenting and cutting of diamond grits result in the breakage of marble.

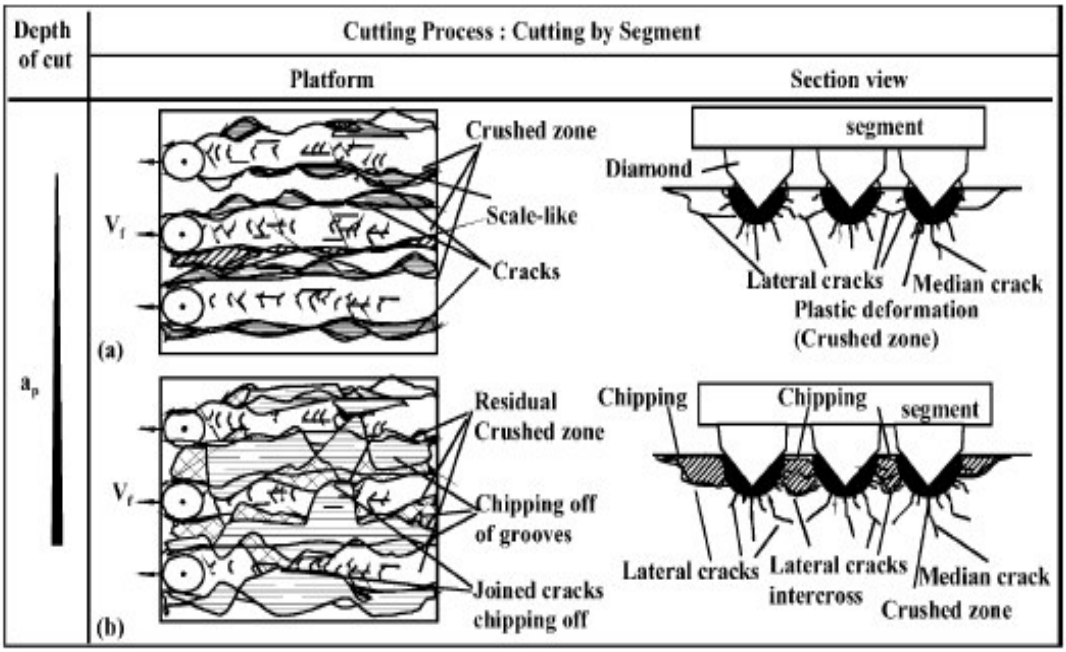

Fig 2.19: Cutting of marble by diamond segments

Thus,

I. Cutting conditions influence fracture deformation and plastic deformation of marble.

II. Only few diamond grits are actually take part in cutting action in case of frame saw.

III. It means cutting process can be effectively done by using single point cutting tool as they gives almost same results.

Luciano Jose´de Oliveira et.al.[8] studied Fe–Cu system (without cobalt addition) as bonding metallic matrix for use in impregnated diamond tools, aiming to process diamond beads with the same performance as the commercial beads. Figure2.20 gives the detail idea about the route they follow,

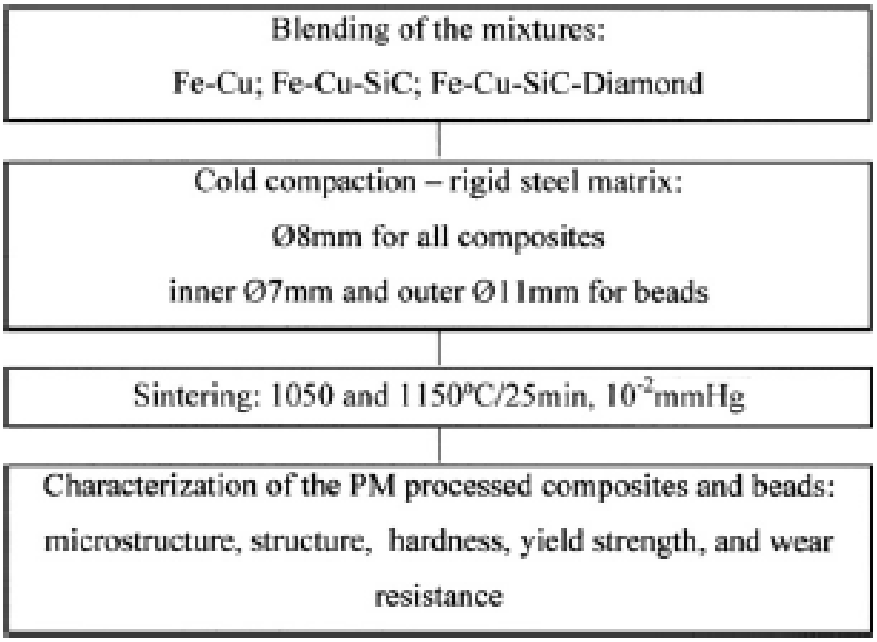

Fig: 2.20: Processing route for diamond beads manufacture, by conventional P/M

The powders were weighed and manually blended according to the compositions Fe–(5–10–15–20)%wt Cu and Fe–(5–10–15–20)%wt Cu–1%wt SiC, via dissolution in chloroform (24h for complete volatilization) using camphor as organic agglomerating/ lubricant (2% volume). SiC was added (1% weight) with the objective to study its

influence in the wear resistance of the alloying matrix. Diamond powder showing specifications of grain size 40/50 mesh (300–425 μm) concentration 50, which account to 13% volume of diamond or 0.44 g of diamond by cm^3. This is the usual diamond concentration in commercial diamond beads.

Powder compaction obeyed two steps:

i. Cold compaction of the Fe–Cu and Fe–Cu–SiC systems, as well as diamond composites in an uniaxial micro alloyed steel matrix, producing cylindrical samples of 8 mm diameter x 8 mm height;

ii. After the ideal Fe–Cu composition, it followed the cold compaction of the diamond beads, in a uniaxial micro alloyed steel matrix of inner and outer diameters of 7 and 11 mm, respectively. In both the cases the applied pressure was of 350MPa.After compaction, the green compacts were placed in furnace for drying at 200 ^{0}C/30 min, under vacuum of 0.013 mbar, aiming to remove the camphor.

The sintering was carried out in a resistive tubular furnace under vacuum of 0.013 mbar, at the temperatures of 1050 and 1150 ^{0}C, to 25 min. it was sintered samples without diamonds for the evaluation of SiC addition influence on mechanical properties of the Fe–Cu system, and for microstructural analysis

Microstructure analyses shows that SiC particles surround the Fe grains, as they accompany Cu liquid flux. At 1150 ^{0}C Cu melts and penetrates into the Fe agglomerates. It forms thin film around Fe particles and promote diffusion.

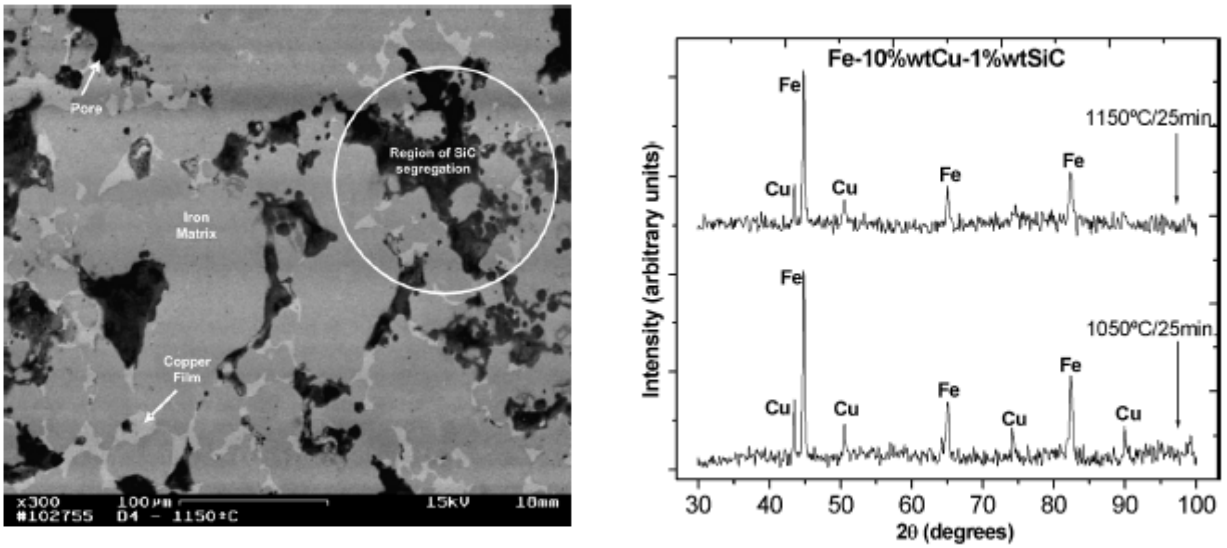

Fig 2.21: SEM micrograph of Fe20%wt Cu-1%wtSiC sample, sintered at 1150 ^{0}C/25 min and XRD patterns of Fe-10%wt Cu -1%wt SiC sample sintered at 1050 and 1150 ^{0}C/25 min.

Higher hardness values found for samples containing more Cu content sintered at 1150^{0}C. Also there is increment in hardness when SiC is added. In case of wear tests figure2.23 shows that there is only small weight loss in all samples. Fe-20%wt Cu–1%wt SiC is the best composition.

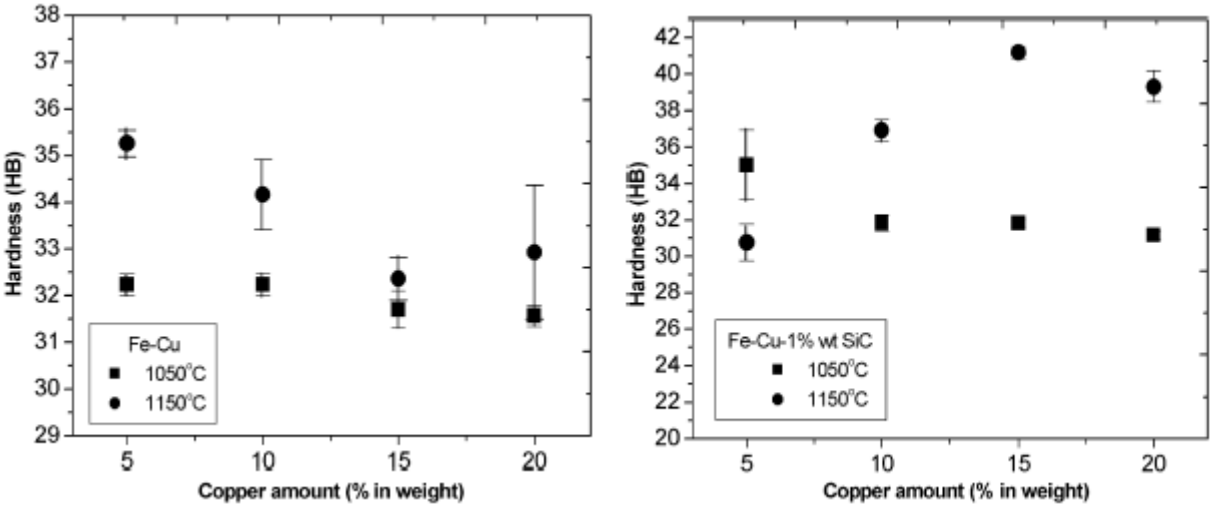

Fig : 2.22: Brinell hardness (HB) values for the Fe- Cu system sintered at 1050 and 1150 ^{0}C.

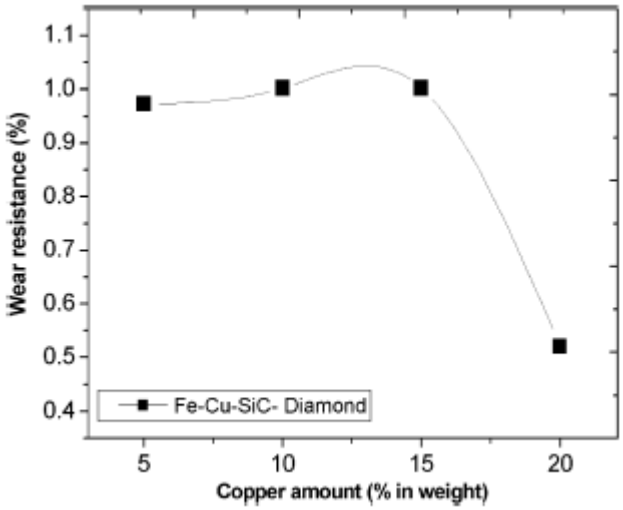

Fig 2.23: Wear resistance of the Fe–Cu–SiC diamond composite, sintered at 1150 ^{0}C/25 min.

Thus, SiC addition promotes an increase by 14% in hardness in the Fe–Cu alloys—which is important since this material acts as a metal matrix wear rate controller. The composition of Fe–20%wt Cu–1%wt SiC–Diamond was the best among the studied ones, because it gives the best results.

2.8: General discussion:

Diamond cutting tool is regularly being used for marbles/ stone cutting. The diamond impregnated matrix primarily consists of Fe, Co and Cu. Cost of tool manufacturing is decided by the cost of the Cobalt powder, which is costlier than other two. There are two ways of manufacturing diamond impregnated tools are visualized -

(1) Prealloyed powder manufacturing by co-precipitation process and (2) Premixing of powders of Fe, Co and Cu. First method is remained a proprictory, hence it has not been developed in India to the best of the knowledge of the author. Second method is being attempted but it needs more in-depth study. Besides this, most commonly used diamond has multi-faceted morphology having sharp edges. Thus it provides efficient cutting action. Other reinforcements like SiC, TiB_2 and WC are finding scope to replace diamond

to some extent. In the context of the present understanding about the DCT, a study is proposed in collaboration with M/s Industrial Metal Powders Pune.

In view of the above technical gaps, the objectives are framed and those are as follows,

1. Material characterization of specimen for components supplied by IMP.
2. To arrive suitable formulation of chemical composition of powders mix by optimizing process parameters of mixes.
3. Material characterization of fabricated specimens.
4. Prototype fabrication of Diamond Cutting tools (DCT).

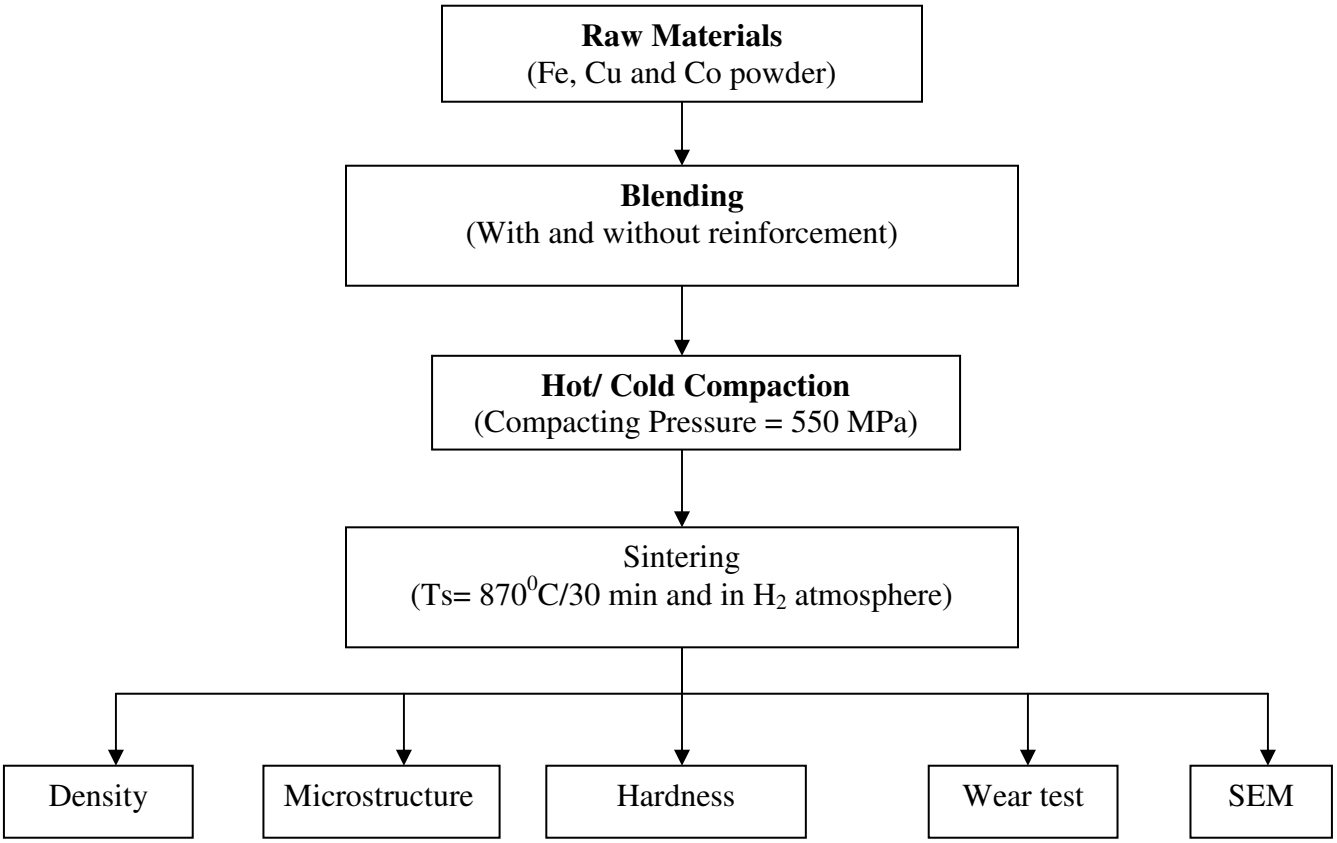

Fig. 2.24: Flow chart proposed to identify important steps in the experimental plan.

CHAPTER-3

EXPERIMENTAL PROCEDURES

3.1 Raw materials:

Based on literature reviews and depend on application Iron, Cobalt, Copper and Tin powders were selected. Reinforcements like WC and Synthetic Diamonds were selected.

Table 3.1.Details of Metal Powders used

Metal powders	Specification	Make
Electrolytic Fe	TR (thermally reduced)grade 8-10 µm	Industrial Metal Powder pvt.ltd
Electrolytic Cu	TR (thermally reduced)grade 8-10 µm	Industrial Metal Powder pvt.ltd
Co	Ultrafine (2-8 µm)	Umicore pvt.ltd. China
Diamonds	Saw grade, synthetic diamonds 2380	China made
WC	7-10 µm T.C.P.	China made

Along with this imported pre-alloyed metal powder of two different grades (A and B) were taken and studied their sintering properties.

3.2 Characterization of powders used:

Powders used for project work were analyzed with respect to following parameters,

3.2.1 Particle size:

Particle sizes for the imported powder was measured by LS Particle Size Analyzer (Make Beckman Coulter LS 13 320) at IIT Bombay, Mumbai. Using this data, particle sizes of all metal powders were selected. Diamond particles size was calculated from micro-structural analysis. Details of report for powder particle size distribution is given in appendix 3.1

3.2.2 Apparent Density:

This characteristic defines the actual volume occupied by mass of the loose powder. Measurement of apparent density is based on the principle of allowing a dry known mass of the powder to fall freely through a standard orifice. Then we got the density by correlation on mass and volume. This measurement was carried out with the help of Hall Flow meter.

Table 3.2: Table showing apparent densities for the powders used in project work

Element	Apparent density (g/cc)
Fe	1.495
Cu	1.20
Co	1.405
Sn	4.143

3.2.3 Chemical Analysis:

Chemical analysis of the imported powders was carried out to find the exact composition of the different elements present in it. This analysis was carried out with respect to Weight percentage. Also instrumental analysis was done in primary stage. Weight analysis gives more accurate results than instrumental.

3.3 Characterization of sintered Materials:

Sintered materials were analyzed with respect to following parameters,

3.3.1 Density Measurements:

Sintered density was calculated by Archimedes Principle. Mass of the sample in air and water was calculated and by using formula given below density was obtained.

$$\rho = \frac{Mass}{Volume} = \frac{m_a}{m_a - m_w} \times \rho_w \text{ (g/cc)}$$

Where, m_a= mass of the sample in air in grams,

m_w= mass of the sample in liquid in grams(i.e. water)

ρ_w= density of liquid used (for water it is 1g/cc)

3.3.2 Hardness Test:

Rockwell hardness tester (FM-700, Make: Future-Tech, Echalkaranji) was used for measurement of hardness on B scale. The flat surface of the specimen is prepared by using polishing paper1/0.A minor load of 10kg in first applied to seat the indenter, and then major load of 100kg was applied for 15 seconds dwell time and resistance to indentation was automatically recorded on the Red color dial gauge.

3.3.3 Wear Test:

The pin-on–disc wear testing machine was used for calculating wear rate of the samples. During testing the pin (i.e. sample) is kept stationary while the circular disc (also known as counter face) was rotated which cause friction between sample and counter face. Alumina disc (165mm diameter) was intentionally used as counter face. The test was performed at room temperature with dry (non-lubricated) condition. The surface roughness of the counter face was maintained by polishing it with 180 grit paper after every test.Acetone was used regularly

before and after test to clean and remove traces of the disc. Initially wear (micron) and frictional force (N) are set to zero and then test begins, as sample gets warned out with respect to time a graph was obtained, which was used for analysis. Also wear rate was calculated by using following formula,

Table 3.3: Specification of the Pin-on-disc machine

Sr. No.	Wear Parameter	Value
1	Rotational Speed	2.1 m/s
2	Track Radius	10 mm to 80 mm
3	Pressure Selected	0.4 MPa
4	Disc Size	Diameter = 165 mm x 8mm thick
5	Software	MAGVIEW-2009
6	Make	M/S Magnum Engineers, Bangalore
7	Disc material	Alumina

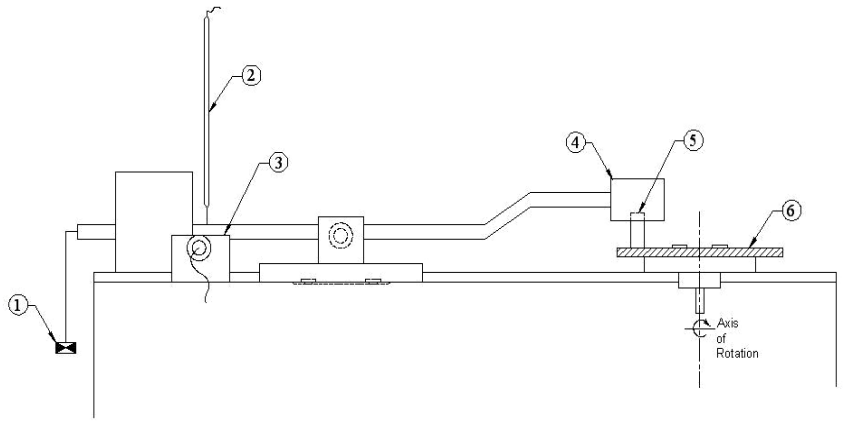

1. Load, 2.Dispalcement Sensor, 3.Load Cell, 4.Specimen Holder (collet), 5. Specimen, 6.Counterface Disc.

Fig.3.1: Schematic of Pin on Disc wear testing machine

3.4 Metallography

Preparation of samples for microstructural analysisbegins with making them absolutely flat by using endless emery belt(340/0)paper. Then specimens were subjected to separate polishing on emery belt starting from 1/0 to 4/0. Samples were turned around 90^0 every time while changing paper. Final polishing was carried out on lapping cloth with alumina powder of soft grade over lapping machine. This whole polishing process helped to gave better and desired surface for microsturctural analysis. Finally samples were etched with freshly prepared 3% Nital for 5 Seconds to reveal all minute micro constituents. Thus, these prepared samples wereanalyzed with Optical and Scanning Electron microscopes.For warned out surfaces analysis samples were just washed with acetone in ultrasonic cleaner and observed under SEM.

3.4.1: Optical Microscopy

In order to analyze the bonding and reinforcement distribution optical microscopy was used. Image analyzer i.e. inverted microscope (Make-CARL ZEISS Germany, Model-Axiovert 40 Mat) with Axiovision LE software was used. This gives the microstructures at 100x, 500 x and 1000x magnification.

3.4.2: SEM/EDS analysis:

In order to analyze the worn out surfaces especially scars and bonding arrangement within the matrix SEM analysis was used. This also helpedto see the morphology of the diamond particles. In SEM, samples are scanned by electron beam which get back-scattered and forms image on screen. Depending on

scattering of electron, image is obtained. EDS (Electro Discharge Spectroscopy) analysis gives the tentative idea about the composition of the elements present in the samples. This can be carried out for a particular point or particular area. Following tables gives the details of SEM specifications.

Table 3.4: Technical specification of SEM

Make	JEOL
Model	JSM 6360 A
Voltage	10 KV
Magnification	30x to 100000x

Table 3.5: Technical specification of the EDS

Instrument	6360(LA)
Acc. Voltage	20.0 kV
Probe current	1.0 nA
PHA Mode	T_3
Real Time	66.51 sec
Live Time	50.0 Sec
Dead Time	25%
Counting Rate	5567 cps
Energy Range	0-20 keV

3.5 Metallurgical investigation of Cutting tools used for references:

Few diamond cutting tools were used for reference purpose. They were characterized for and results were considered as a bench mark. Following flow chart will help to provide necessary information about this investigation.

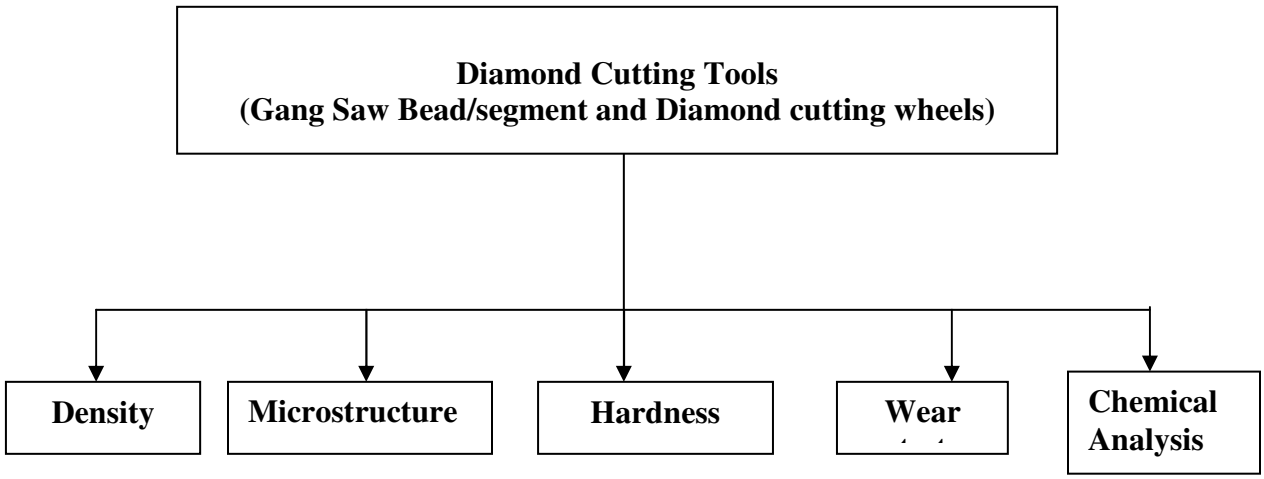

Fig.3.2: Flow chart showing characterization of DCT

3.6 Fabrication of Diamond Cutting Tools at lab Scale

Samples are fabricated through following procedure,

3.6.1 Powder mixing:

Mechanical mixing of powders of different compositions was blended by using conical shaped blender.The blends contained different powder composition taken as weight percentage.

3.6.2: Compaction:

Compaction of premix was carried out at different pressures from 400 MPa to 600Mpa by using Universal Testing Machine (UTM of capacity 10 tons). L/D

ratio for samples was maintained less than 1 (L/D<1) accordingly dies and mass was selected. Unidiractional compaction was carried out at room temperature for laboratory experiments while hot compaction was used for making prototype. Force was calculated by using basic formula as Pressures= Force/Area. Compacted green samples were handled delicately and shifted to tubular furnace for sintering operation.

3.6.3: Sintering Furnace:

Tubular furnace (max Temp. 1200^0C) with a provision for necessary reducing or inert atmosphere works as a Sintering furnace. Samples were placed in heating zone and heated to its sintering temperature (Ts=0.4 Melting Point). The same furnace was used for in- situ Infiltration and sintering technique. H_2 gas was used to provide necessary reducing atmosphere. At the end of outlet of furnace the H_2 gas was burned and then released in a atmosphere. N_2gas was used for flushing the other gases at the beginning and at the end of the sintering. Table 3.5 gives the details of the sintering parameters used.

Table 3.6: Parameters used for sintering process

Sr.No.	Sintering Parameters	Values
1	Sintering temperature	Up to 1100^0C
2	Sintering time	From 5 min to 60 min
3	Cooling way	Till 500^0C cooled in a furnace with controlled atmosphere and further cooling in air
4	Atmosphere used	H_2 and N_2 (10:90)
5	Gas pressure	0.5-1kg/cm^2
6	Gas flow rate	100-200 ml/min

3.7 Infiltration process:

For getting more densification in sintered products infiltration technique is generally used. In other words it can be said that for achieving more density in sintered components infiltration process is used.

In this process infiltration of metal having lower melting point than those other metals was infiltrated in to the compact at higher temperature (i.e. temperature higher than its melting point). Two pallets/compacts were made one of basic matrix and other of metal which had to be infiltrated. Infiltrated metal pallet was placed below base matrix pallet and they were placed in a sintering furnace and sintered. At higher temperature pores of the compacts got openedand molten metal due to capillary action was sucked into those pores, filled them completely which ultimately helped to increase density as well as helped to increase bonding strength also. In this case there was nothing but in situ infiltration and sintering happened. For the present project work two types of infiltration was used, Cu-infiltration and Cu-Sn or bronze infiltration.

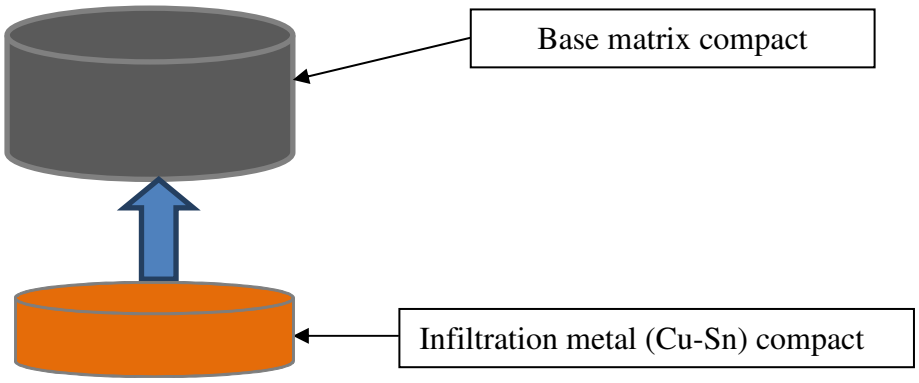

Fig. 3.3: Schematic of Infiltration Process

3.7.1 Cu-infiltration:

At sintering temperature of 1150^0C, cu-infiltration was successfully used. This gave the expected increase in density as well as hardness also. From density of compact made without infiltrate respective porosity was calculated. This calculation was used to find out exact mass required for infiltration. That mass of Cu powder was taken and compacted.

3.7.2 Cu-Sn (Bronze) infiltration:

It was revealed that for diamond cutting tools the temperature more than 850^0C will deteriorate the synthetic diamonds, in other words it increases graphitization. Thus to lower down sintering temperature from 1150^0C to range of 800-850^0C we mixed tin powder to Copper in ratio of 25:75. This ratio was considered from equilibrium diagram of Cu-Sn which ultimately helped to lower down sintering temperature up to 830^0C.

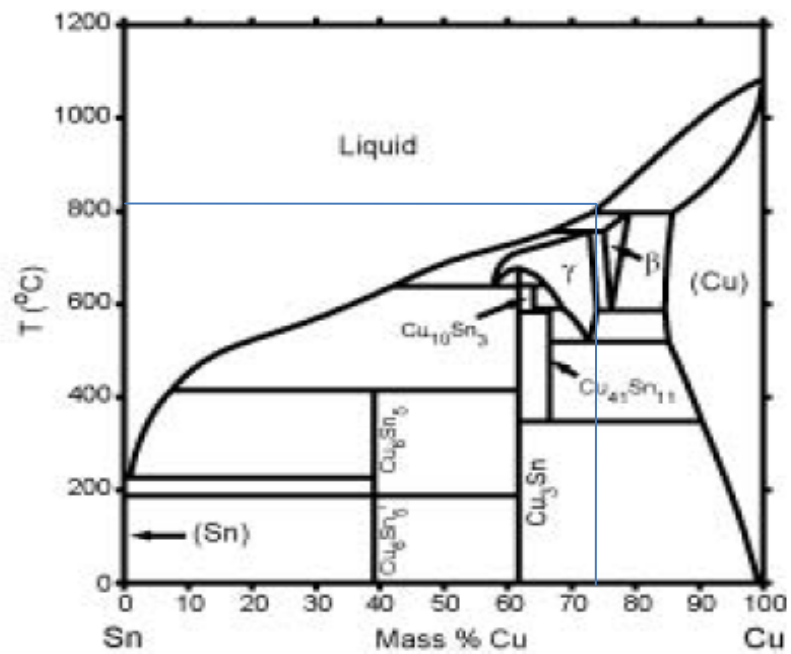

Fig: 3.4 Sn-Cu Equilibrium diagram [3]

3.7.3: Formulae used for amount of infiltrate required:

$\rho_{th} = \rho_{Fe\,Co} = (f_{Fe} \times \rho_{Fe}) + (f_{Co} \times \rho_{Co})$

$P = 1 - (\rho_s / \rho_{th})$ ---------- (1)

Vol. of Compact = in mm^3 ---------- (2)

Vol. fraction of porosity = Eq^n 1 X Eq^n 2= Vol. of infiltrate in mm^3

$\rho_{infiltrate} = (m_{infiltrate} / \text{Vol of infiltrate})$

$m_{infiltrate} = (\rho_{infiltrate} \times \text{Vol of Infiltrate}) \times 10\%$ extra ---------- -- (3)

where,

ρ_{th} : theoretical density of composite

ρ_s : sintered density of composite

$m_{infiltrate}$: mass of infiltrate

Equation 3 will give exact mass of infiltrate required.

3.8 Prototype Tool Fabrication:

Final prototype tool was manufactured by Super Cut Tool Manufactures, Mumbai.. All parameters were selected as per industrial convenience for making tool and it was tested further. Repetitive prototype manufacturing and testing was carried out to check reliability of the process.

Table 3.6: Parameters used for prototype tool manufacturing

Sr.No.	Parameters	Values
1	Initial compacting pressure at room temperature	300 kg/cm^2
2	Sintering temperature	810^0C
3	Sintering time (soaking time)	3 min
4	Compacting pressure during sintering process (Hot- Press sintering)	20 kg/cm^2
5	Atmosphere used	Normal

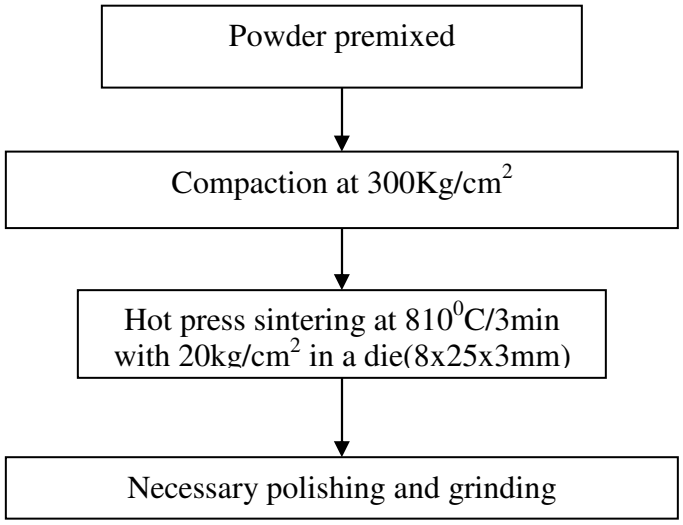

Fig: 3.5 Flow diagram showing prototyping method for DCTs manufacturing

CHAPTER 4

METALLURGICAL INVESTIGATION OF DIAMOND CUTTING TOOLS AND PRE-ALLOYED POWDERS

Metallurgical investigation of Diamond Cutting Tools (DCTs)

Diamond cutting tools used in the local market were supplied by the industrial metal powders Pvt.ltd (IMP) Pune for metallurgical investigation. There were two types of diamond cutting tools provided viz. a) Circular disc and b) Segment of Gang saw bead. Other category of the powder was produced by co-precipitation technique and presently being imported by the diamond cutting tool manufacturer.

4.1 Segment of Gang Saw:

Segment of Gang Saw (SGS) was analyzed using various tests to understand the metallurgy of fabrication. The preliminary findings of the segment are summarized as follows,

4.1.1: Chemical composition

The SEM-EDS was used to estimate approximate chemical composition of the elements as mentioned in Table 4.2 and corresponding spectrum is given in Table 4.1. However, it could not detect Co due to the limitation of the EDS.

Table 4.1: EDS analysis for SGS

Elements	Fe%	Cu%	Co%	Sn%	Zn%
Wt%	56.03	37.75	----	4.29	0.98

4.1.2: Microstructures

Figure 4.1 shows diamond particles embedded in the alloyed matrix. These diamond particles are mostly irregular hexagonal shape having sharp edges. All these diamond particles are in range of 50-60 µm.

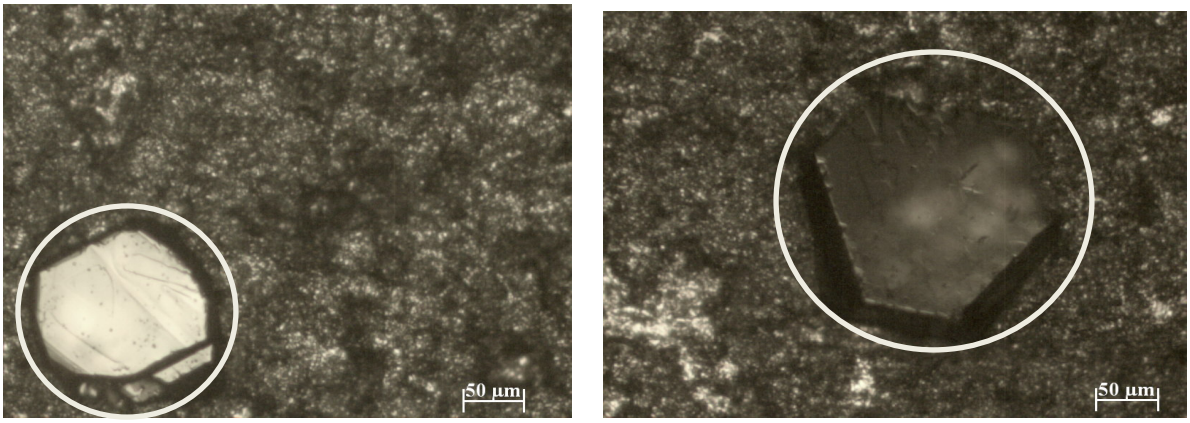

Fig: 4.1: Microstructures of SGS: encircled objects showing diamond particle**.**

4.1.3: Measured properties of SGS

Three segments of gang saw were studied for preliminary properties and those are given in Table 4.1.

Table 4.2: Observations of the SGS

Sr. No.	Parameters	Observations
1	Dimensions	15 x 24 x 10 mm
2	Sintered Density	7.328 g/cc
3	Hardness	75.35 HRB
4	Wear Rate	$4x10^{-4}$ mm^3/m

4.2: Diamond Cutting Wheel

Schematic of Cutting wheel used for analysis is shown in Fig. 4.2. The outer part of the wheel having teeth like projection is made by the sintering process and contains diamond particles. This part was made separately and then brazed to the steel base material.

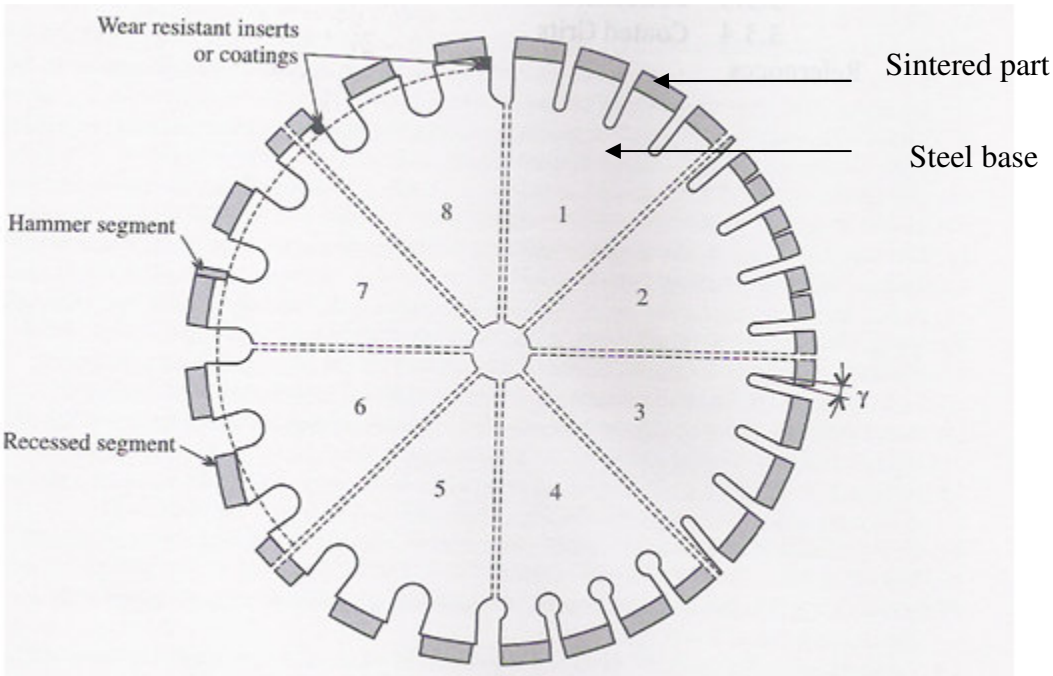

Fig: 4.2 Schematic of Diamond Cutting Wheel used for analysis

4.2.1: Chemical analysis

It is revealed from Table 4.2, sintered part of the cutting wheel was made up of copper base material and other elements in smaller quantity. Copper material was brazed to the periphery of the cutting wheel while the base material was analyzed as mild steel whose composition is shown in Table 4.3.

Table 4.3: SEM-EDS analysis of Sintered part of Cutting wheel

Elements	Fe%	Cu%	Co%	Sn%	Zn%	Cr%	W%
In Wt%	9.18	65.00	----	16.99	8.19	0.10	0.54

Table 4.4: Instrumental analysis of Steel base of Cutting wheel

Elements	C%	Mn%	Si%	S%
In Wt%	0.58	0.64	0.20	0.015

4.2.2: Microstructures

Base of the cutting is typical medium carbon steel depicts spheroids of carbides in ferritic matrix as shown in Fig.4.3 whereas sintered part show do not indication of any well developed phases in the matrix as evident from Fig.4.4.

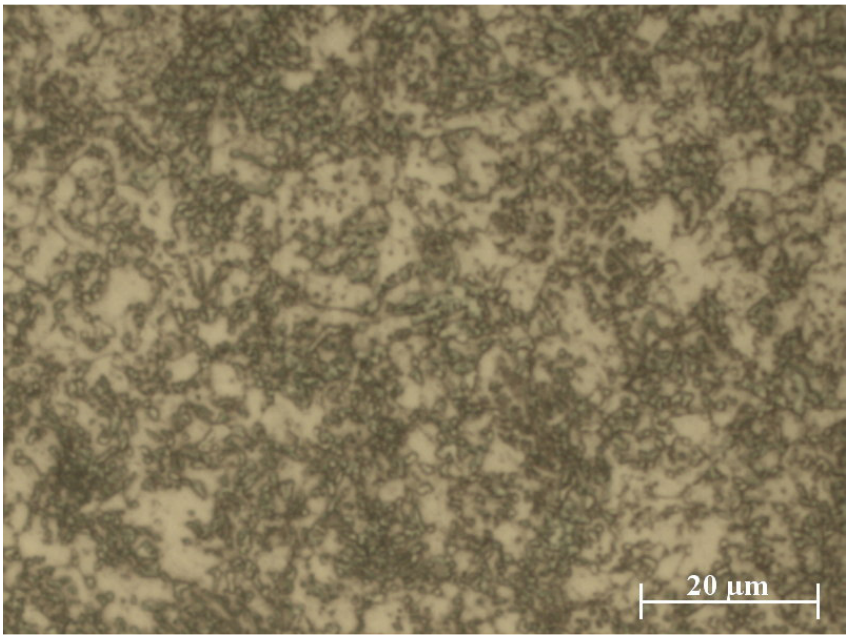

Fig: 4.3: Optical microstructure of steel base material of cutting wheel showing spheroidal structure obtained at 100x magnification

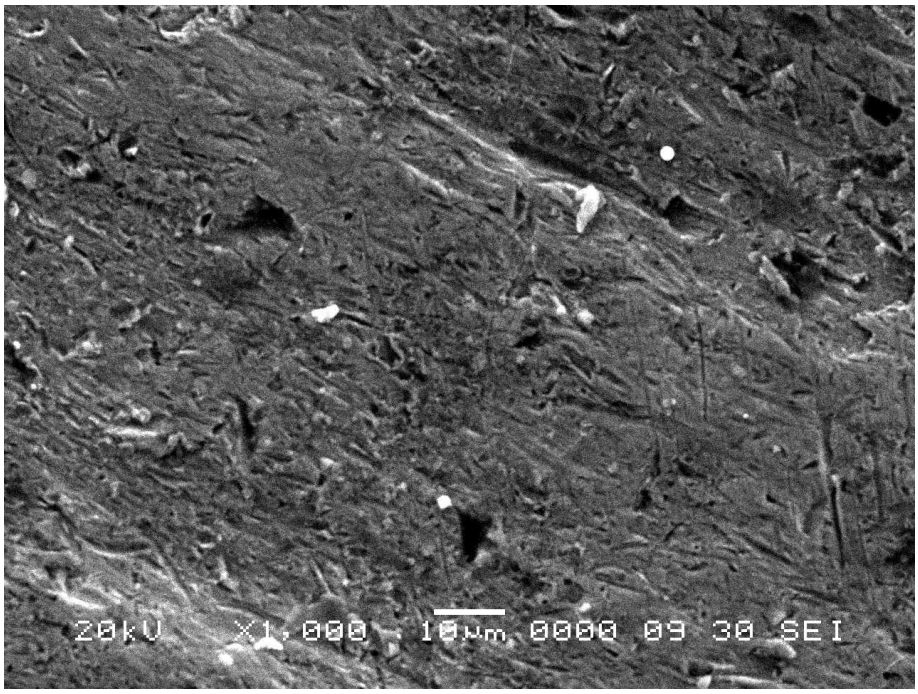

Fig: 4.4: SEM image of Sintered part of cutting wheel.

4.2.3: Measured properties

The sintered part of the cutting wheel was tested for hardness study**.** Table 4.4 gives micro hardness readings for sintered part.

Table 4.5: Micro hardness values for sintered part of cutting wheel

Reading No.	Micro hardness in HV Load=100g Dwell time =15sec
1	151.3
2	150.3
3	147.6

4.3 Analysis of Pre-alloyed powder available in market:

There were two types of powders were provided by the IMP and designated as A and B. Both these powders are believed to be produced by co-precipitation technique.

4.3.1: Chemical Composition

The SEM-EDS was used to estimate approximate chemical composition of the sintered specimen for the sample-A and Sample-B and the weigh analysis of the same is given in Tables 4.5 and 4.6 and their corresponding EDS spectrum is given in Figure 1.1 in Appendix 1

Table 4.6: EDS and chemical analysis for pre-alloyed powder A

Type of analysis	Chemical composition in wt%						
	Fe	Cu	Co	Cr	W	Zn	Sn
SEM-EDS	25.99	39.93	22.26	0.14	0.24	0.30	0.04
Weigh Chemical analysis	25.13	41.56	25.92	-	-	-	-

Table 4.7: EDS and chemical analysis of Pre-alloyed powder B

Type of analysis	Chemical composition in wt%						
	Fe%	Cu%	Co%	Cr%	W%	Zn%	Sn%
SEM-EDS	16.04	55.15	21.92	0.04	0.36	0.33	-
Weigh Chemical analysis	18.50	55.40	26.31	-	-	-	-

4.3.2: Sintering of Pre-alloyed powder compacts

Two types of Pre-alloyed powder (without diamond reinforcement) was compacted and sintered as per the process parameters indicated in Table 4.3.

Table: 4.8: Parameters used for making sintered compacts

Sr.No.	Parameters	Observations
1	Compacting pressure	400 MPa and 550 Mpa
2	Sintering temperature	870^0C
3	Soaking time	30 min
4	Atmosphere	H_2 :N_2 (10:90)
5	Cooling	Cooled in furnace till 500^0C with reducing atmosphere and further cooled in air.

4.3.3: Microstructures

Microstructures of Sample A and B show uniform distribution of phases with no visible porosities. Figures 4.4 and 4.5 show magnified images by SEM indicates islands of copper infiltrated uniformly during sintering in the entire matrix.

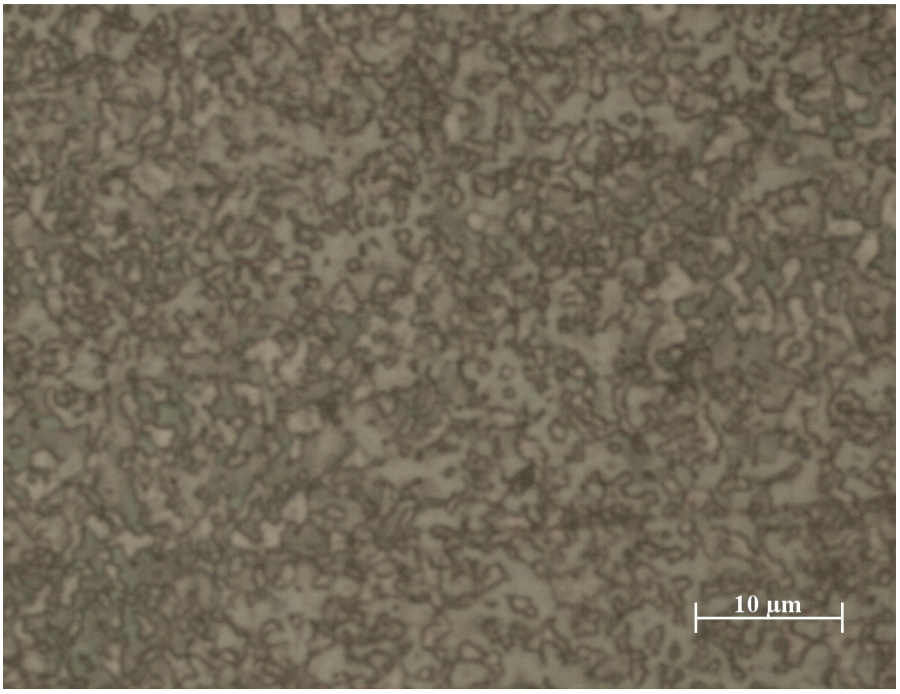

Fig.4.5: Uniform microstructure of Sample A (500x)

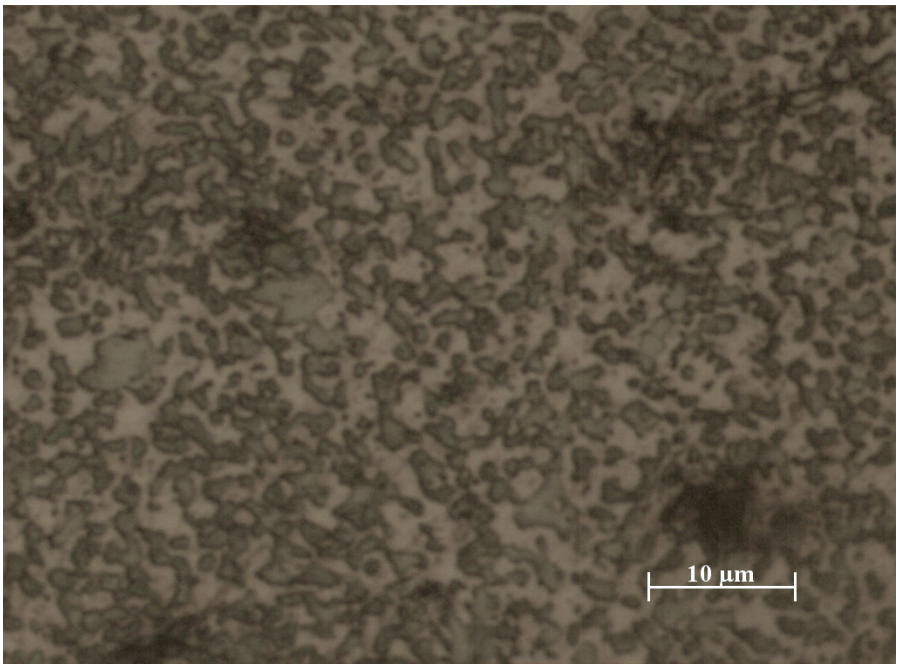

Fig.4.6: Uniform microstructure of Sample B (500x)

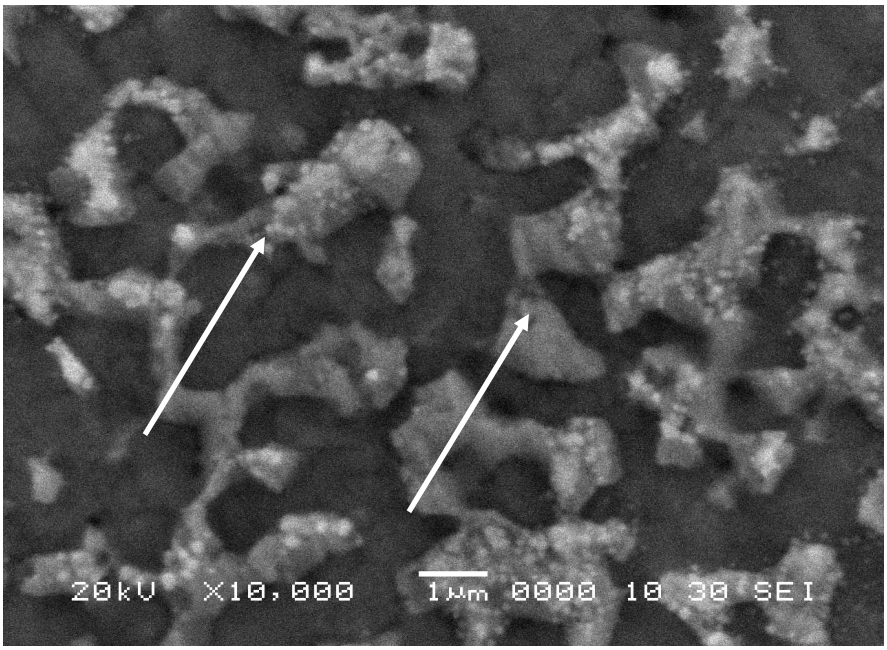

Fig. 4.7: SEM image of Sample Arrows showing islands of copper

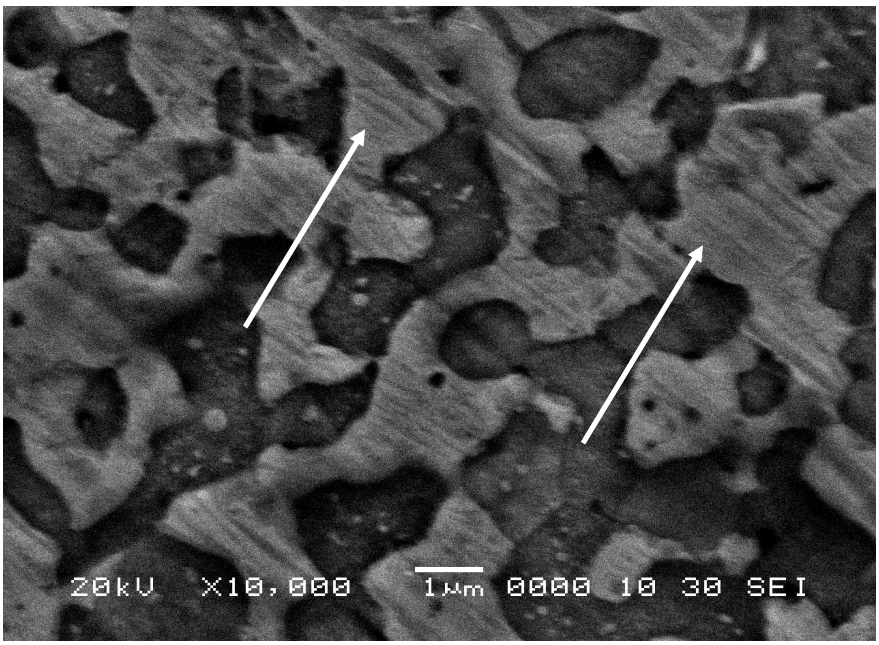

Fig 4.8: SEM image of Sample B showing islands of infiltrated copper

4.3.4: Measurement of properties

Characterization of Samples A and B are indicated in Table 4.4. It is observed that the hardness and sintered density increases with compacting pressure, but wear rate remains slightly affected.

Table 4.9: Showing different values of test results for different compacting pressure

Parameters	Compacting pressure 400MPa		Compacting pressure 550MPa	
	Sample A	Sample B	Sample A	Sample B
Sintered density (g/cc)	8.1878	8.4047	7.923	8.415
Hardness (HRB)	94.6	82.2	96	84.46
Wear Rate (mm^3/m)	0.00120	0.00297	0.001623	0.001683

4.4 General observations:

In the present work, three types of materials (Diamond cutting tools and prealloyed powder) were used for metallurgical investigation. Based on the analysis, the following observations can be drawn-

a) Segment of gang saw was primarily made of iron and cobalt and other low melting constituents which are used for achieving densification by liquid phase sintering.

b) Diamond cutting wheel is primarily copper based with diamond impregnated sintered at the rim of the cutting wheel.

c) Pre-alloyed powder contained iron, cobalt and other elements like copper, tin for achieving densification by liquid phase sintering.

CHAPTER 5

RESULTS AND DISCUSSION

After going through the metallurgical investigation as outlined in chapter 4 on existing DCTS and well known pre-alloyed powders, an independent study was initiated to arrive at an optimum chemical formulation of the powder blend. Other emphasis was on use of indigenous electrolytic iron powder by replacing carbonyl iron powder and to optimize the content of cobalt whose fluctuating market prices drives the cost of fabrication of DCT.

5.1 Sintered characteristics of individual powders:

Individual sintered compact of Copper, iron and Cobalt was investigated. The summary of the results is shown in Appendix 5. It is observed that increasing sintering temperature, increases density and hardness considerably in copper and iron sintered compact whereas there is marginal effect of pressure on sintered properties of cobalt as shown in Figs.5.1 and 5.2. However, it is seen that sintered density of copper and iron gradually increases with increasing sintering temperature (920°C) whereas hardness of copper falls at 450MPa. Thus fall in hardness of copper at 920°C temperature may be due to grain coarsening [2]. It was typically seen in all three materials transverse crack surfaced at 550 MPa while making green compact. This phenomenon is normally seen when compacting pressure goes beyond compressibility of powder.

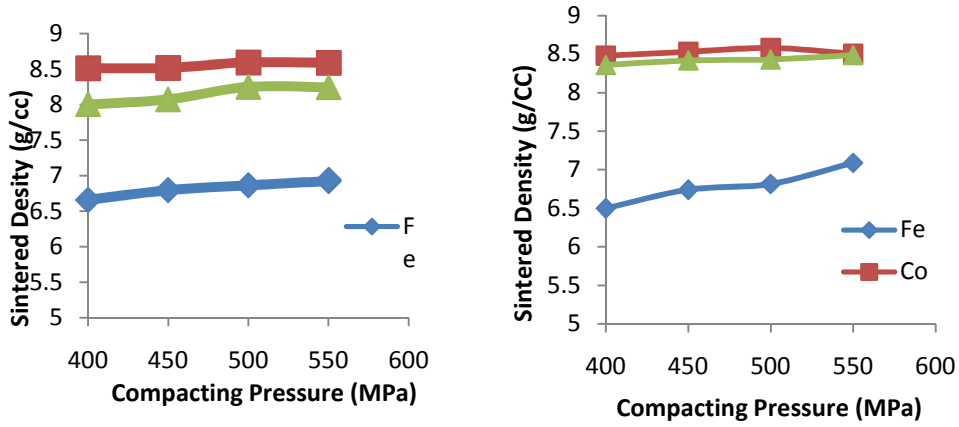

(a) (b)

Fig: 5.1: Effect of compacting pressure on variation in sintered densities of individual sintered compacts (a) sintered at 870^0C (b) sintered at 920^OC

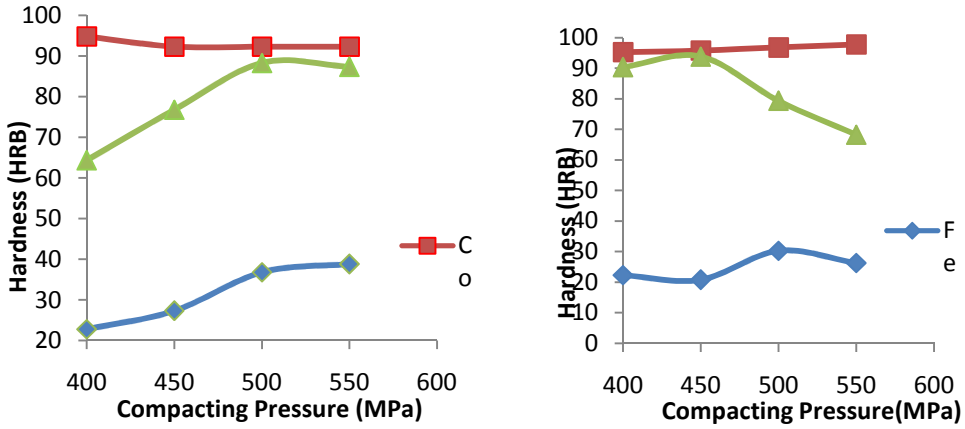

(a) (b)

Fig: 5.2: Effect of compacting pressure on variation in hardness of individual sintered Compacts (a) sintered at 870^0C (b) sintered at 920^0C

5.2 Optimization of chemical composition:

Based on the understanding from the earlier chapter on investigation of well established pre-alloyed powders and chemical composition of DCTS, two types of a premixed blend, as given in Table-5.1, of electrolytic iron powder, cobalt and copper were taken for optimization of sintering parameters and sintered properties of the compacts.

Table 5.1: Showing details of results obtained for premixed powder (without diamond)

Ex. No.	**Composition (% by weight)**		
	Fe	Cu	Co
4	27	45	28
5	19	55	26

5.2.1: Optimization of sintering process

Two compositions of premixed powder blends (Table 5.1) were taken as given by Expts 4 and 5 and these compacts were subjected to different optimization cycles. It is essential to know the optimum properties of the resulting compact by varying sintering time, sintering temperature and compacting pressure. Few experiments were conducted to ascertain the effect of individual process parameters on properties of sintered compacts.

5.2.1.1. Optimization of sintering time

Sintering time was varied from 5 min to 60 min by keeping compacting pressure 550MPa and sintering temperature 870^0C unchanged. It is evident from Fig.5.3 (a, b) that maximum sintered density and hardness achieved at 30 min of sintering time. However, minimum wear rate is seen at 45 min of sintering time as shown in Fig.5.3 (b). It is noticed that copper content is bit high in Expt. 5 than Expt.4 which gives rise in sintered density, decrease in wear rate with marginal change in hardness. Copper has strong adhesive forces which help the matrix to reduce wear rate reasonably than Expt.4.

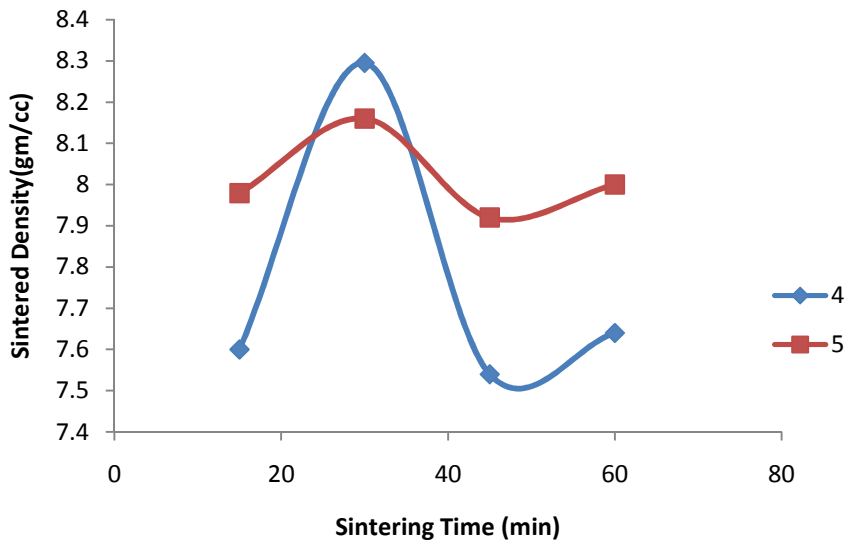
8.4
8.3
8.2
8.1
8
7.9
7.8
7.7
7.6
7.5
7.4
Sintered Density(gm/cc)
0
20
40
60
80
Sintering Time (min)
4
5

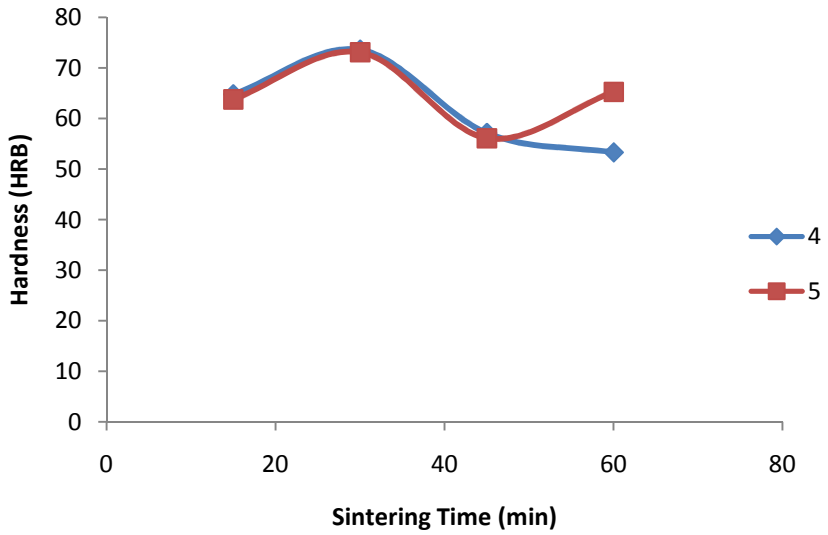
80
70
60
50
40
30
20
10
0
Hardness (HRB)
0
20
40
60
80
Sintering Time (min)
4
5

(a)

(b)

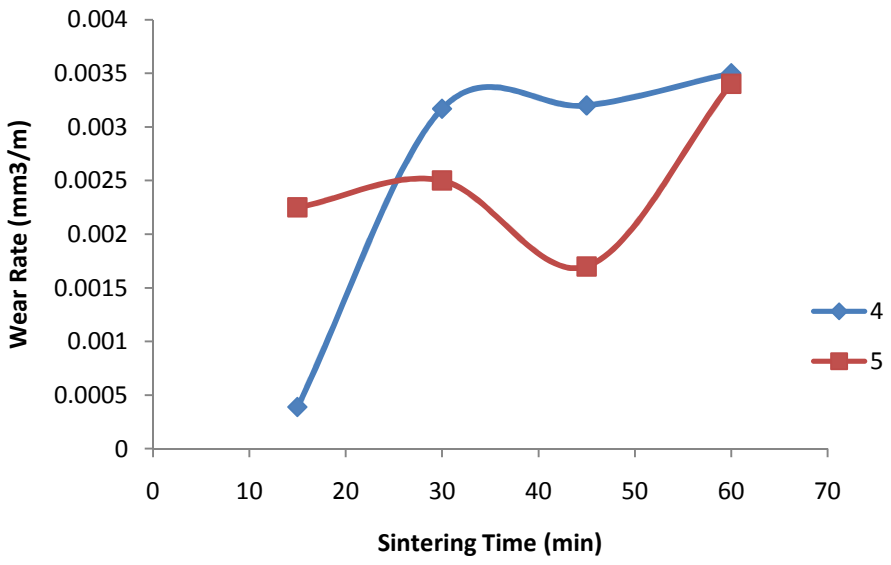

(c)

Fig.5.3: Effect of sintering time on (a) sintered density, (b) hardness, and (c) wear rate (Expts. 4 and 5)

5.2.1.2. Optimization of sintering temperature

Two sintering temperatures are chosen for optimization to study the properties of the sintered compacts while other parameters viz. compacting pressure (550 MPa) and sintering time (30 min) remained constant during the process. It is observed that sintered density and hardness decreases with increasing sintering temperature whereas wear rate increases with increasing sintering temperature as depicted in Fig.5.4.

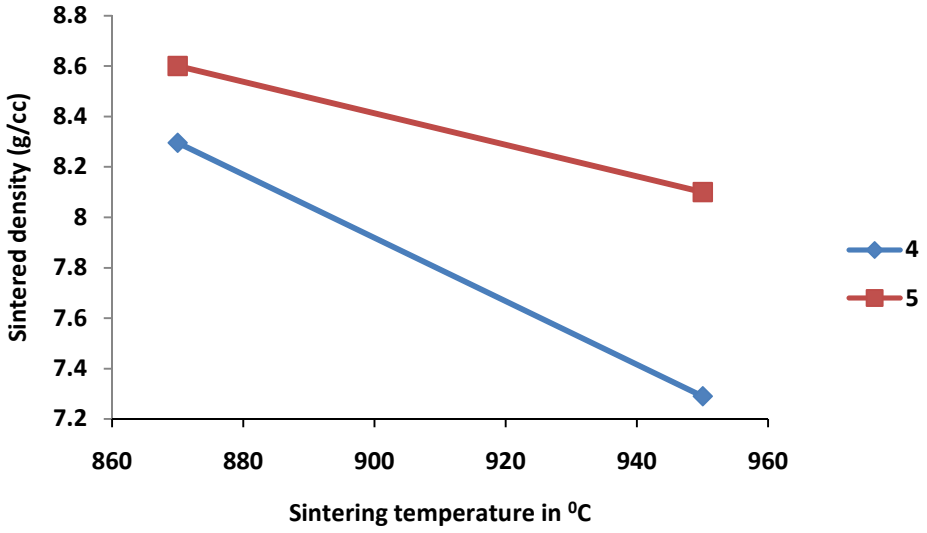
8.8
8.6
8.4
8.2
8
7.8
7.6
7.4
7.2
Sintered density (g/cc)
860
880
900
920
940
960
Sintering temperature in ⁰C
4
5

(a)

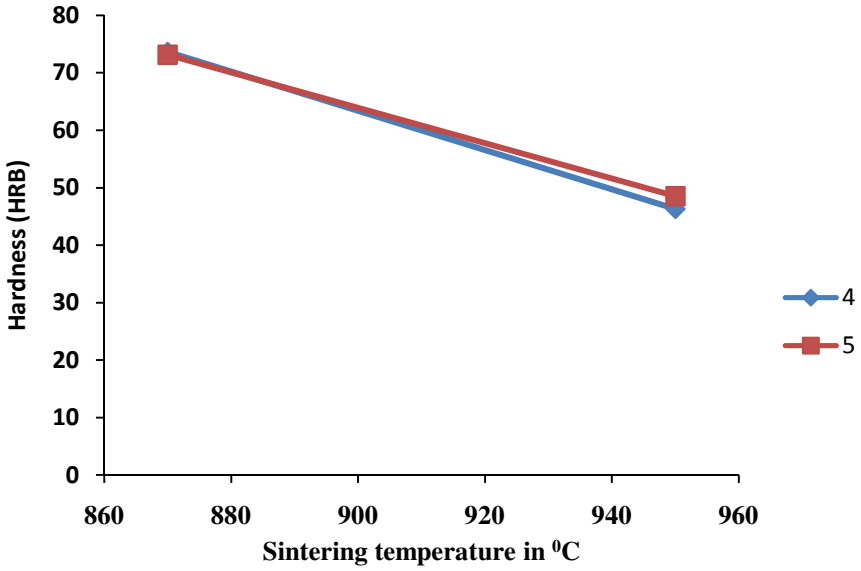
80
70
60
50
40
30
20
10
0
Hardness (HRB)
860
880
900
920
940
960
Sintering temperature in ⁰C
4
5

(b)

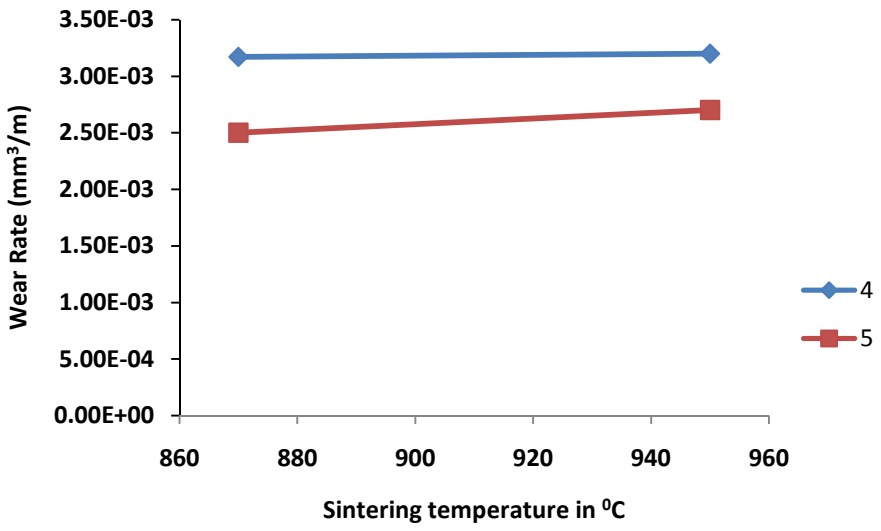

(c)

Fig.5.4: Effect of sintering temperature on (a) sintered density, (b) hardness, and (c) wear rate (Expts. 4 and 5)

5.2.1.3. Optimization of sintering pressure

Two sintering pressures were taken for optimization while other parameters viz. sintering temperature (870°C) and sintering time (30min) were kept constant. It is observed from Fig. 5.5 that sintered density, hardness and wear rate decreases with increasing compacting pressure. At higher pressure (600 MPa), green compacts showed transverse surface cracks due to excessive pressure beyond the compressibility of the powder blend. Overall sintered density of Expt.5 is on higher side than Expt.4 due to more amount of copper content.

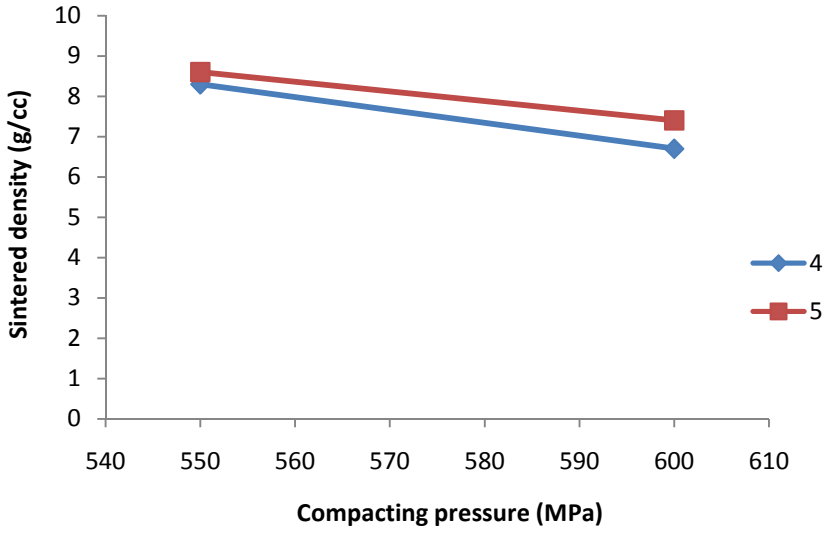
Sintered density (g/cc)
10
9
8
7
6
5
4
3
2
1
0
540
550
560
570
580
590
600
610
Compacting pressure (MPa)
4
5

(a)

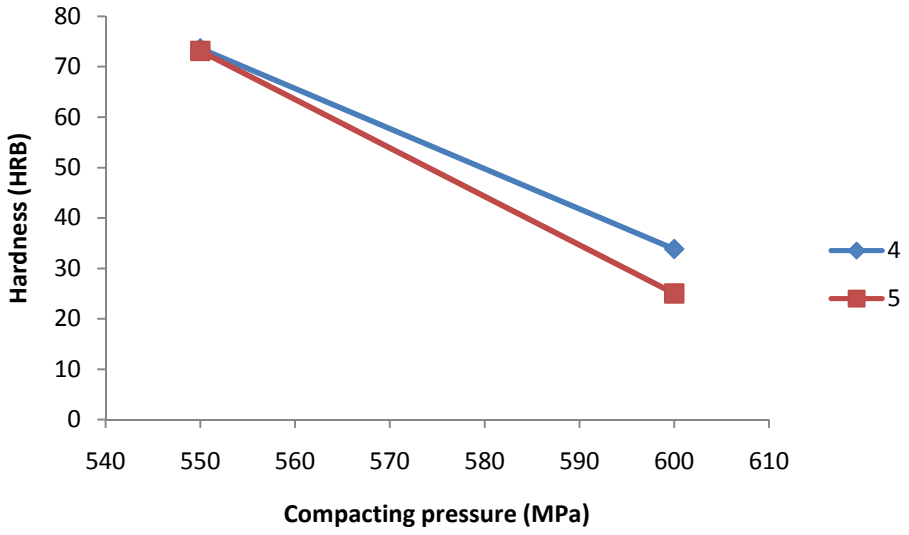
Hardness (HRB)
80
70
60
50
40
30
20
10
0
540
550
560
570
580
590
600
610
Compacting pressure (MPa)
4
5

(b)

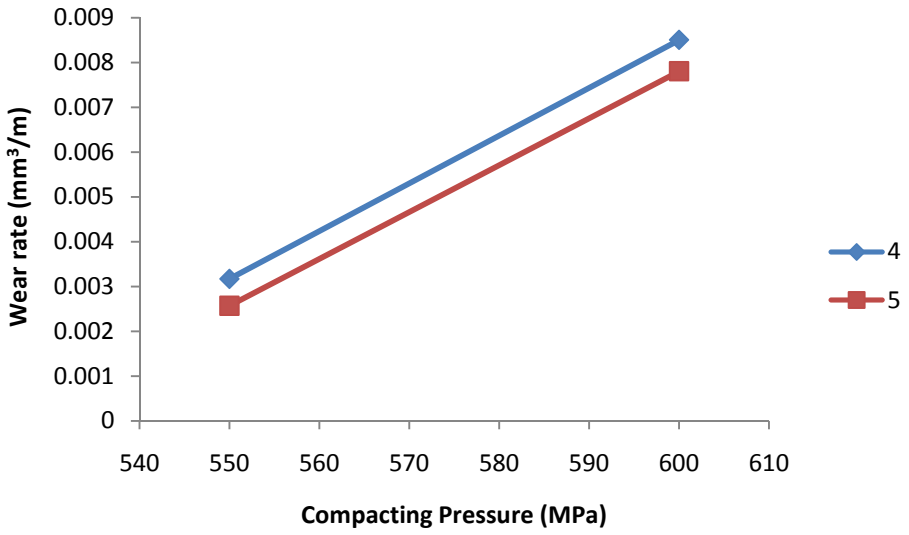

(c)

Fig.5.5: Effect of compacting pressure on (a) sintered density, (b) hardness, and (c) wear rate (Expt No. 4 and 5)

From the forgoing discussion, the optimum process parameters identified are a) Compacting pressure 550MPa, b) Sintering temperature 870^0C and c) sintering time 30 min.

Observations on some premixes

Having identified sintering parameters for the premixed powders, then next step was to evaluate the need of Co content and that was varied in between 10 to 20% in some of the experiments. Few experiments were conducted and their results of the experiments are given in Table 5.2. In order to get general understanding of cobalt, few experiment with arbitrarily blend of powders containing atomized iron powder of Hoganas, imported prealloyed powders and electrolytic iron powder of IMP were tried. It is observed that minimum wear rate was noted in Expt.6 that is in close proximity to Expt.11 and Expt.10. Thus premix made out of electrolytic iron powder with less cobalt can give rise some level confidence in development of diamond cutting tools. However, copper as liquefied

agent might not be adequate enough to give fully densified structure. Hence it was suggested to resort for external infiltration to improve density further.

Table.5.2: Details of experiments carried out for optimizing Co content
P= 550MPa, Ts=870^{0}C/30min.

Ex. No.	Composition (% by weight)			Sintered density (g/cc)	Hardness (HRB)	Wear Rate (mm^3/m)	Remarks
	Fe	Cu	Co				
6	30	60	10	6.96	73.37	0.001532	Premixed powder of Fe, Cu, Co
7	40	50	10	6.760	42.14	0.009070	Premixed powder of Fe, Cu, Co
8	50	40	10	6.750	85.14	0.01510	Premixed powder of Fe, Cu, Co
9	27	45	28	7.54	81.45	0.0051	50% of Hoganas Fe powder + 50% IMP Fe powder (premixed)
10	40	40	20	7.845	94.00	0.002922	Premixed powder of Fe, Cu, Co
11	25.13	41.56	25.92	8.3885	87.70	0.001219	Prealloyed powder prepared by co-ppt method in IMP lab

5.3 Selection of Infiltration Process:

Infiltration process is explained schematically as shown in Fig. 3.3. During sintering process temperature rises and reached till the melting point of infiltrate and thus it gets absorbed into the pores of the green compact by capillary action. Appropriate selection of infiltrant based on its melting point decides the sintering temperature. In this particular work, pure copper and Cu-Sn system is attempted

5.3.1: Cu-infiltration

The effect of copper infiltration was seen in few experiments as given in Table 5.4. It has significant influence on hardness and improved dense structure. Copper infiltration was attempted on Iron –Cobalt system wherein Fe: Co ratio of 3:1 was maintained and the resultant green compacts were made at 550 MPa and sintered at 1150^{0}C for 30 min. The relative comparison is shown in Table 5.3 for copper infiltrated and without copper

infiltrated. In next few experiments amount of cobalt was reduced to explore optimum condition by studying their characterization.

Table 5.3: Comparison of sintered properties (550 MPa and 11500C/30min)

Parameters	Fe-75% ,Co-25% (without copper infiltration)	Fe-75%, Co-25% (with infiltration)
Expt. No.	12	13
Sintered Density (g/cc)	6.65	8.044
Hardness (HRB)	68	87
Wear Rate (mm^3/m)	0.0033	0.00254

5.3.2: Cu-Sn (Bronze) infiltration

Purpose of using low melting point like Cu-Sn infiltrant was suggested to overcome three important limitations viz. a) to reduce sintering temperature, (b) protect the synthetic diamond from graphitization as it undergo graphitization beyond 950^oC and (c) save precious thermal energy required for sintering. The selection of Cu-Sn containing 75% Cu and 25%Sn respectively was chosen to initially to understand extent of improvements. Few experiments with Cu-Sn alloy were tried as mentioned in Table 5.5. The corresponding liquidus temperature of Cu-Sn alloy is 800^0C as shown in Fig. 3.4.

5.3.3: Optimization of Cobalt content

The iron-cobalt system was extensively studied to get optimum properties. Co was varied from 5 % to 25% (by wt) and blended with electrolytic iron powder. These experiments were carried out with two types of infiltrate viz. Cu and Cu-Sn as discussed in earlier section. Tables 5.4 and 5.5 show results of some experiments conducted at 1150^oC using copper infiltration whereas other experiments were conducted at 950^oC using Cu-Sn infiltration. It is observed that minimum wear rate is seen at 15% Cobalt and its corresponding microstructure depicts highly densified structure as shown in Fig. 5.6.

Table.5.4: Effect of Co on Fe-Co system using Cu- infiltration process

Ex. No.	Composition (% by weight)		Sintered density (g/cc)	Hardness (HRB)	Wear Rate (mm^3/m)	Sintering temperature (^oC)
	Fe	Co				
13	100	0	7.958	87.8	2.9E-03	1150
14	95	5	7.8158	74.8	3.7E-03	1150
15	85	15	8.004	77.8	3.3E-03	1150
16	75	25	8.044	84.3	2.5E-03	1150
17	0	100	8.84	58.3	3.0E-03	1150

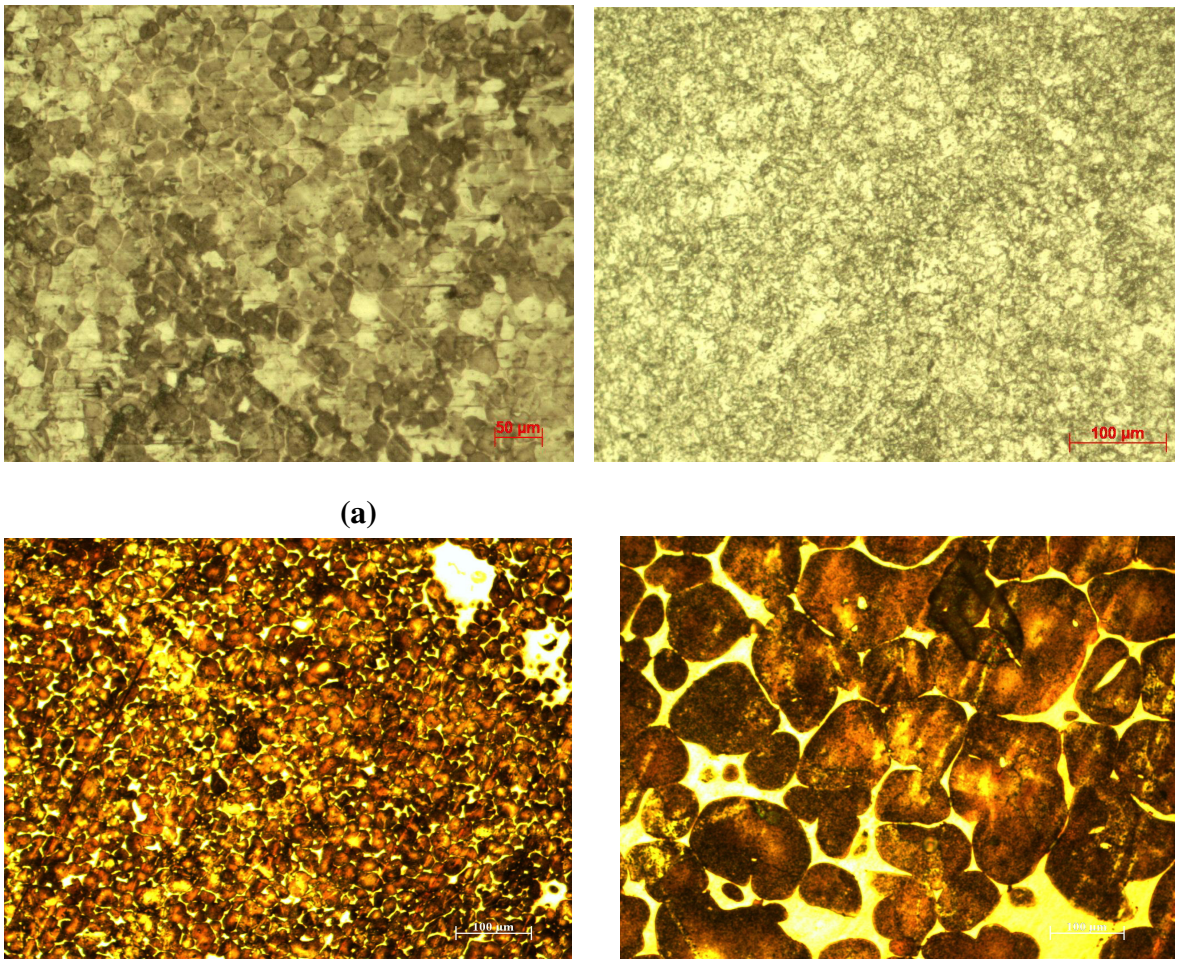

Fig: 5.6: Microstructures for (a) Pure Fe with Cu-infiltration at 100x (b) Pure Co with Cu-infiltration at 100 x (c) 85-15 (Fe-Co) with Cu- infiltration at 100 x (d) at 500x

Table.5.5: Effect of Co on Fe-Co system using Cu- Sn infiltration process, Ts= 950^0C/30min

Ex No.	Composition (% by weight)		Sintered density (g/cc) for infiltration	Density (g/cc) Without infiltration	% porosity Without infiltration	Hardness (HRB) for infiltration	Wear Rate (mm^3/m) for infiltration
	Fe	Co					
24	100	0	8.10	6.32	18.97	88	2.0E-03
25	95	5	7.98	6.45	17.83	89.8	3.4E-03
26	85	15	8.04	6.76	15.18	92.3	2.0E-03
27	75	25	8.17	6.89	14.62	96.3	3.7E-03

It may be interesting to note that microstructure show visible porosity without infiltration and fully dense structure when Cu-Sn infiltration is done as revealed from Fig.5.7.

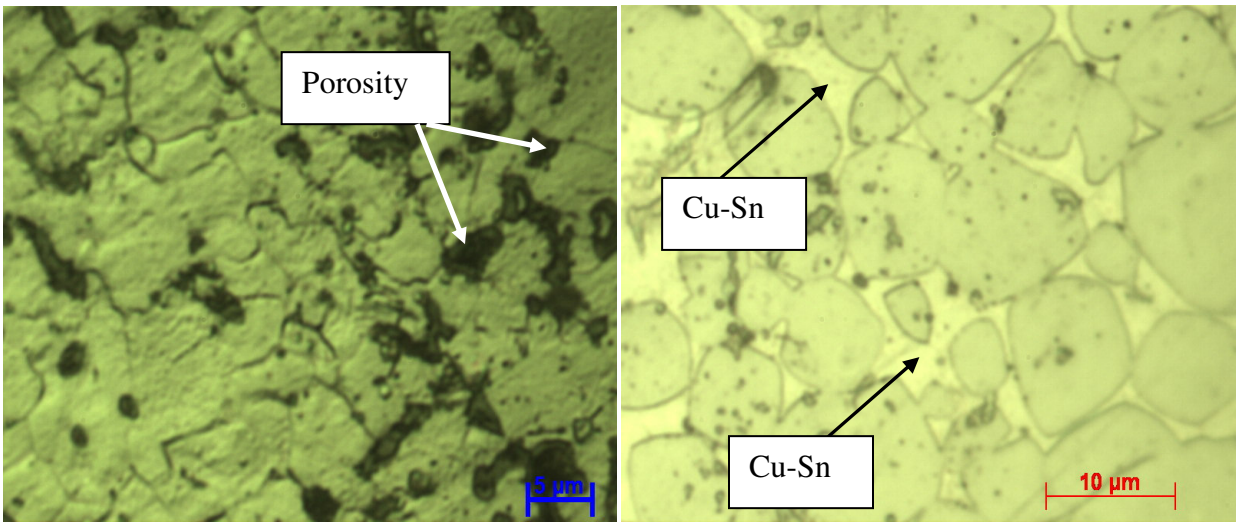

(a) **(b)**

Fig.5.7: Optical microstructure of Fe with 15%Co (a) without infiltration shows porous structure (b) Cu-Sn infiltration shows fully dense structure

5.3.4.2. Measured properties comparison

Sintered properties of Fe-Co system with and without infiltration are analyzed as function of cobalt content. It is evident from Figs. 5.10 (a and b) that sintered density and hardness gradually increases with cobalt content. However, there is definite transition noted at

15% Co content for minimum wear rate as indicated in Fig.5.8c. Beyond this threshold value, there is dramatic increase in wear rate. Overall it shows Cu-Sn infiltration gives positive effect on improving sintered properties.

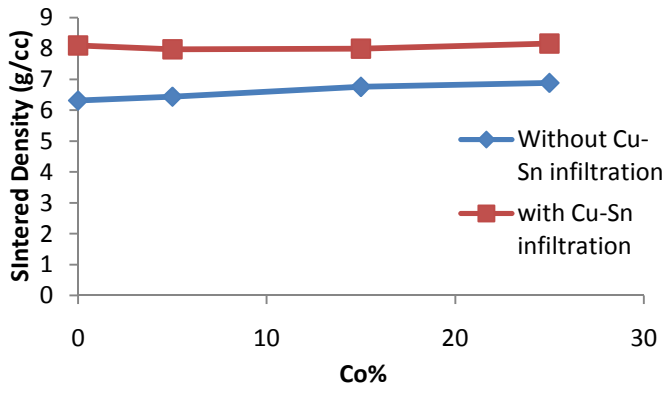

(a)

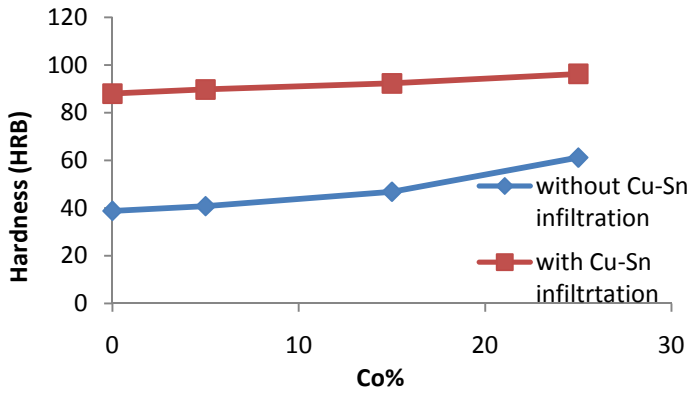

(b)

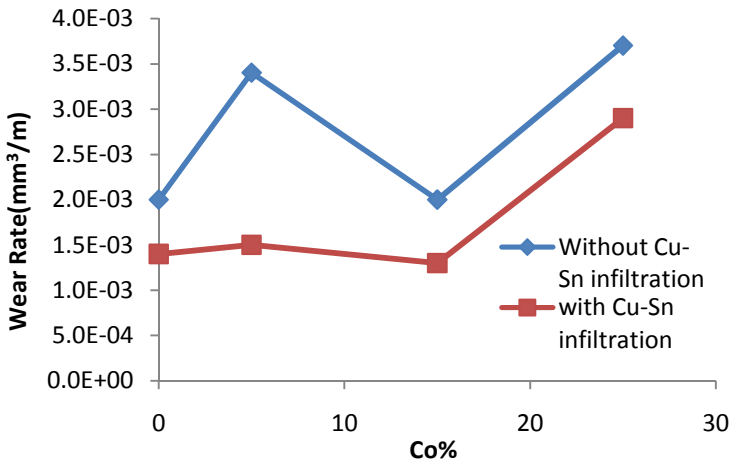

(c)

Fig.5.8: Effect of cobalt content on sintered properties (a) on sintered density, (b) Hardness and (c) Wear rate

5.4 Effect of reinforcements :

After optimization of cobalt content in the iron matrix which amounts to 15%Co, the next step was to realize the impact of reinforcements typically tungsten carbide (WC) and synthetic diamonds on wear resistance of the matrix. Normally synthetic diamonds of 50-70 µm and WC (TCP-5-7 micron) are added to the tune of 2 to 5%. Using these reinforcements, few experiments were conducted as shown in Table 5.5.

Table 5.6: Effects of reinforcements on Fe-Co system by using Copper infiltrate and Cu-Sn infiltrate

Ex. No.	**Composition (% by weight)**				**Sintered density (g/cc)**	**Hardness (HRB)**	**Wear Rate (mm^3/m)**	**Sintering conditions**
	Fe	Co	Diamonds	WC				
18	100	0	2	-	7.34	99.3	8.4E-04	1150/30 min
19	100	0		2	8.2	94.3	2.9E-03	1150/30 min
28	100	0	2	-	7.8	85.8	2.4E-03	950/30 min
29	95	5	2	-	7.75	89.8	2.6E-03	950/30 min
30	85	15	2	-	7.859	91.3	1.2E-03	950/30 min
31	75	25	2	-	7.909	95.8	4.8E-03	950/30 min
32	85	15	5	-	7.56	89	1.2E-03	850/30 min
36	85	15	2	-	7.729	92.3	3.6E-03	850/30min
37	85	15	2	2	7.83	91.8	1.4E-03	850/30min

Figure 5.9 shows fully dense microstructure with 2% Diamonds dispersed in the matrix. But diamond surface is covered with thin coating of Cu-Sn alloy which might have occurred sintering process.

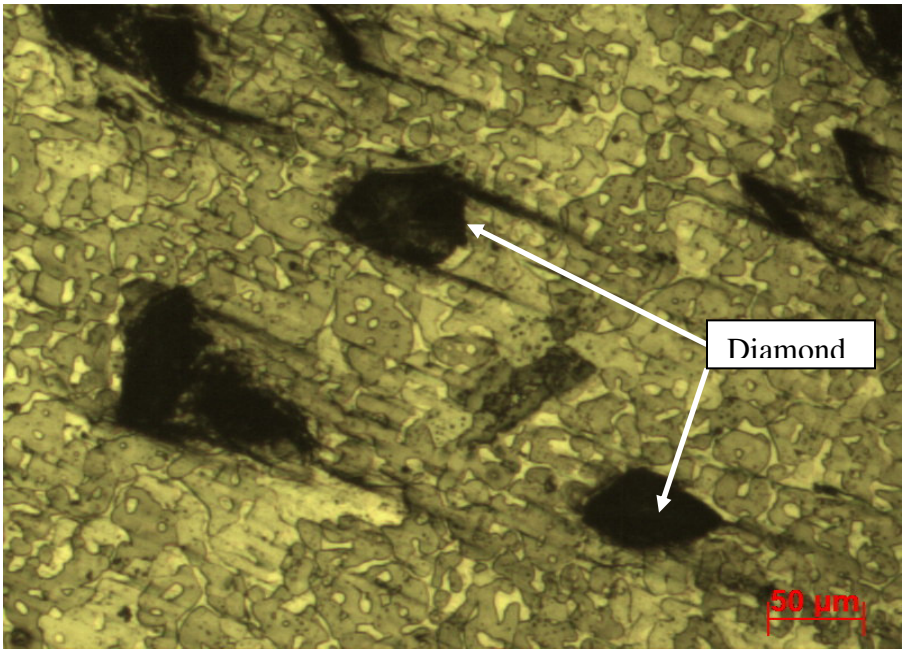

Fig: 5.9: Microstructures of 15% Co and 2% Diamonds (50-70 microns) with Cu-Sn infiltration depicts diamonds covered by Cu-Sn coating (Expt No. 37)

It is quite obvious from Fig.5.10 that addition of diamonds affect sintered density considerably whereas hardness is marginally affected which may due to weak particle – matrix interface. However, wear rate is minimum at 15% Co in case of diamond reinforced matrix.

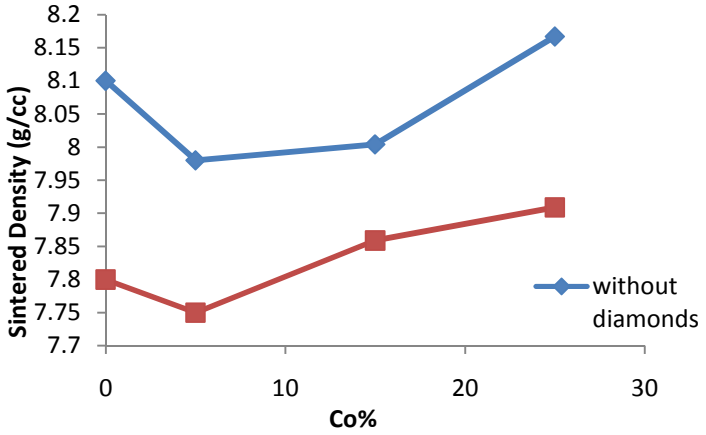

(a)

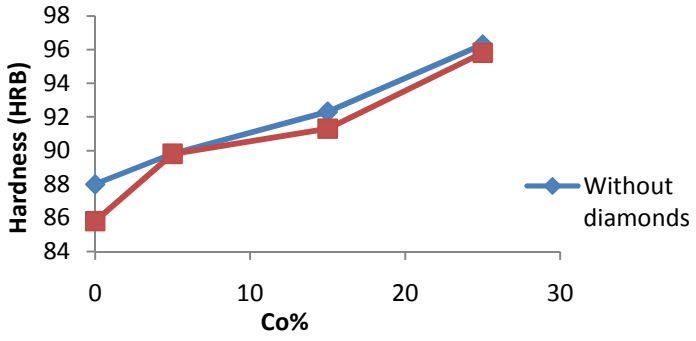

(b)

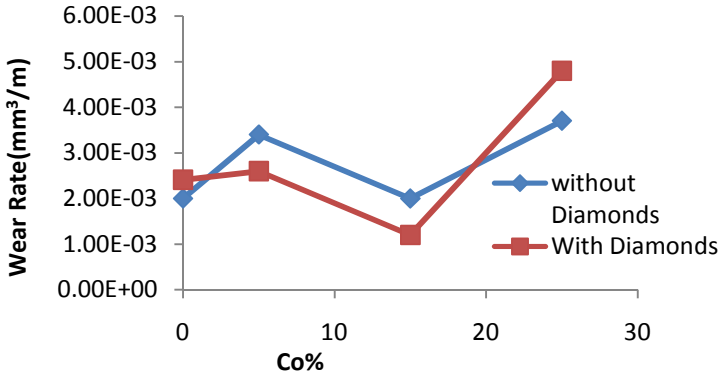

(c)

Fig. 5.10: Comparison between with and without diamond reinforcement using Cu- Sn infiltration process (Grade 3830 (50-60) diamonds were used)

Sintering behavior of in-situ infiltrated matrix

In order to realize the effect of in-situ infiltration, few experiments with Cu-Sn infiltrant was tried on Fe-Co system containing 15% Co. Table 5.7 gives overall average content of cobalt estimated as 8.9%. The sintered compacts showed bulging and some indication of transverse cracks on bulged surface a shown in Fig.5.11.

Table 5.7: Sinter-ability of premixed powder with reinforcements

Ex. No.	**Composition (% by weight)**					**Sintered density (g/cc)**	**Hardness (HRB)**	**Sintering conditions**
	Fe	Co	Cu	Sn	Diamonds			
33	50.46	8.9	28.12	9.315	3.125	5.7514	38.8	850/30min
34	50.46	8.9	28.12	9.315	3.125	6.558	45.8	850/15min
35	50.46	8.9	28.12	9.315	3.125	6.620	46.13	850/5min

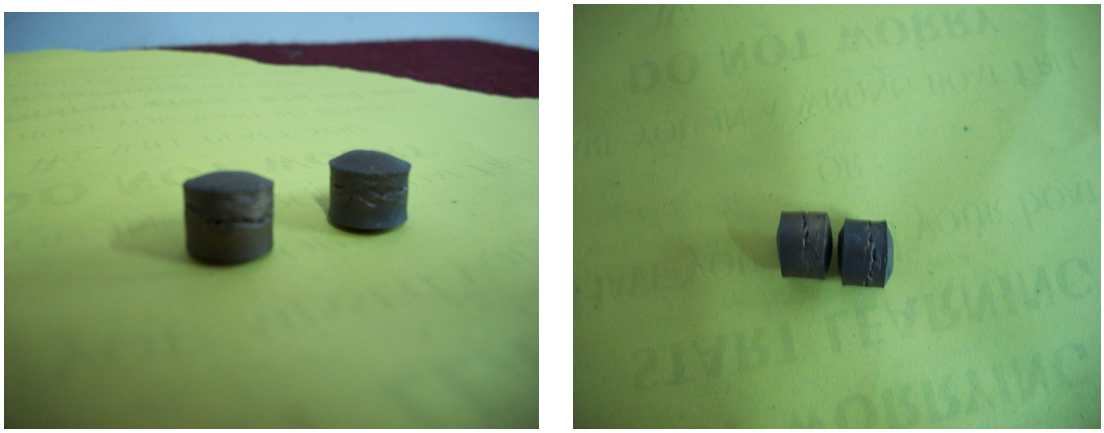

Fig: 5.11: Bulged and Cracked samples fabricated using premixed powders

5.5 Prototyping of DCTs:

It was learnt from earlier experiments on premixed powder with in-situ infiltration process adopted at laboratory level did not meet the expectation of industry on developed formulation of DCTs as given in Table 5.7.

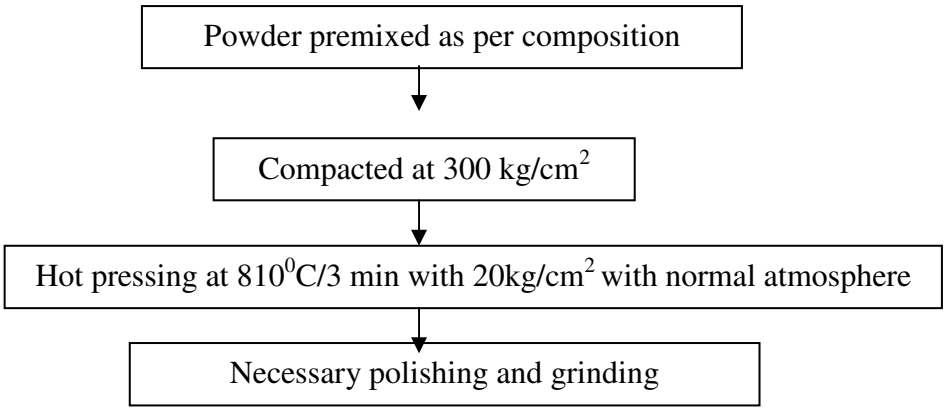

Fig.5.12: Flow chart explaining details of fabrication steps adopted

While transferring knowledge gained at lab scale level to industrial level, it was necessary to have repeatability and reproducibility in the process of DCTs fabricated in accordance to the practice adopted at Industry level (Fig. 5.14). Hence three successive trials were proposed for each composition. Table 5.9 gives details of the successive trial were taken on the composition containing 9.32% Sn. But all those tools were successfully fabricated except sweating of bronze liquid on surface of DCTs at 830°C. In the next set of experiments wherein tin content was reduced to 5% and thus using this formulation, again three successive trials were taken with reduced sintering temperature of 810°C. All these fabricated tools did not show any sweating of the liquid and no operational difficulty noticed. By reducing Sn content to 5%, it is noticed that density has gone up slightly but hardness reduced few points. However, wear rate shows marginal variation. In order to increase the hardness of DCTS for 5%Sn, additional successive trials were taken with 15% Cobalt and 5%WC separately by other parameters unchanged.

Table- 5.8: Optimum formulations obtained at lab scale study

Experiments	Composition by %weight					
	Fe	Co	Cu	Sn	Diamonds	WC
Composition for Expts 39,40,41	48.22	8.52	28.12	9.37	2.88	2.88
Composition for Expts 42,43,44	48.22	8.52	32.49	5.00	2.88	2.88

Table 5.9: Industrial trials of fabrication of DCTs

Expt. No.	Description	Density (g/cc)		Hardness (HRB)		Wear Rate (mm^3/m)	
	9.32% Sn	Max	Min	Max	Min	Max	Min
39	Trial 1	7.2	7.13	95.3	95.13	0.00017	0.000083
40	Trial 2	7.2	7.12	95.16	93.13	0.000047	0.000066
41	Trial 3	7.26	7.16	96.6	95.8	0.000027	0.000083
	Avg.	**7.22**	**7.13**	**95.68**	**95.35**	**0.000081**	**0.000077**
	5% Sn						
42	Trial 1	7.78	7.68	91.8	90.8	0.00024	0.000086
43	Trial 2	7.85	7.56	91.8	90.46	0.00021	0.000081
44	Trial 3	7.84	7.72	94.23	92.46	0.000046	0.00009
	Avg.	**7.82**	**7.65**	**92.61**	**91.24**	**0.000165**	**0.000085**

Heterogeneity of the DCTs

The summary of the average results of the trials are given in Table 5.9. It is quite clear that the wear rate is exceptionally low which is attributed primarily the role of diamond in reducing the wear rate of the parent matrix. Similar observation is noticed in density and hardness in the results of successive lots. Since diamond is mechanically added in the blend of powders, some level of non uniformity is inherently present in the matrix. Therefore, certain statistical variation is seen in wear properties for the same composition of the diamond cutting tools. Figure 5.13 show diamond particles embedded in the alloyed matrix. The variation in the data can also expressed in terms of standard deviation in hardness, density and wear rates as given in Fig.5.16. Microstructures (Fig.5.13) of these tools show clearly diamond particles with sharp cutting edges. Worn surface

analysis of control specimen (SGS) as shown if Fig.5.15 shows severely deformed surface giving an indication of delamination wear mode where as worn (Fig.5.16 and 5.17) surface of fabricated DCTs containing 9.37% Sn and 5% Sn shows smooth deformed surface giving an impression of delamination wear mode

Table 5.10: Summary of results in ranges for successive trials drawn from Table 5.9

DCT composition	**Density (g/cc)**	**Hardness (HRB)**	**Wear Rate (mm^3/m)**
For 5% Sn	7.65-7.85	91.24-92.61	$0.85x10^{-4}$-$1.65\ x10^{-4}$
For 9.32% Sn	7.13-7.22	95.35-95.68	$0.775x10^{-4}$-$0.815x10^{-4}$

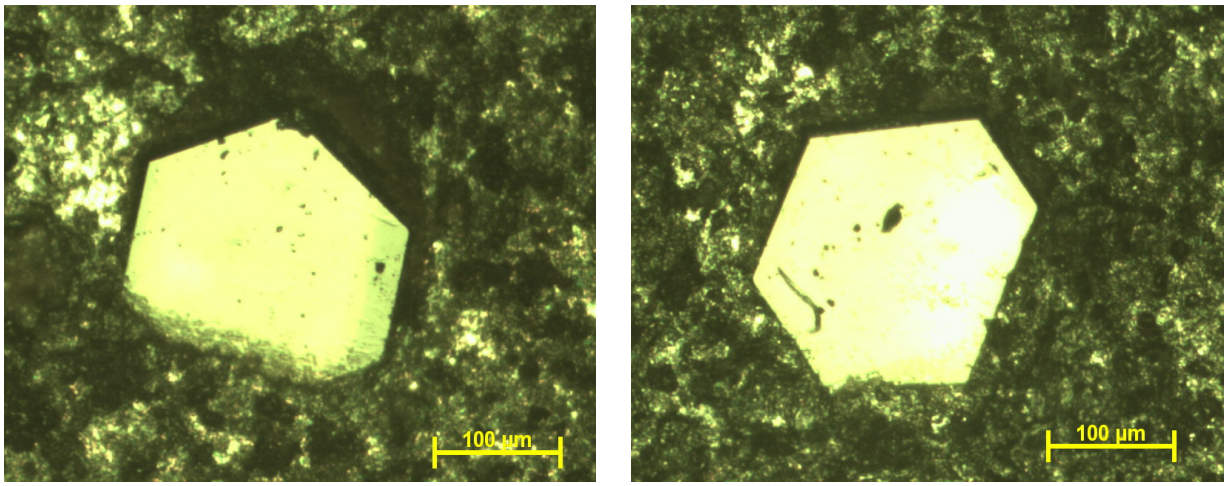

Fig.5.13: Microstructures showing diamond particles in the alloyed matrix at 100x

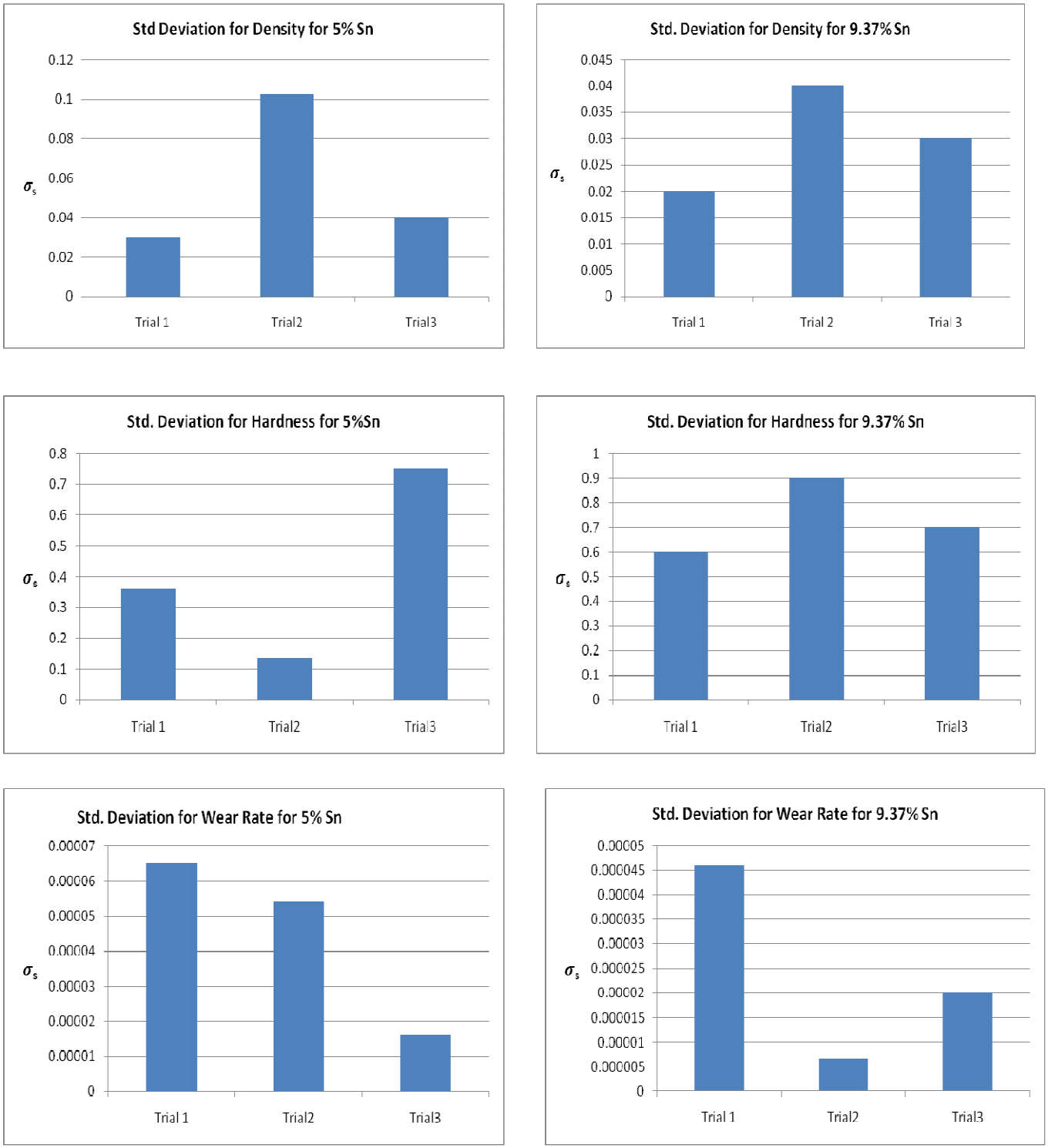

Fig 5.14: Standard deviation for trials for 5% Sn and for 9.37% Sn

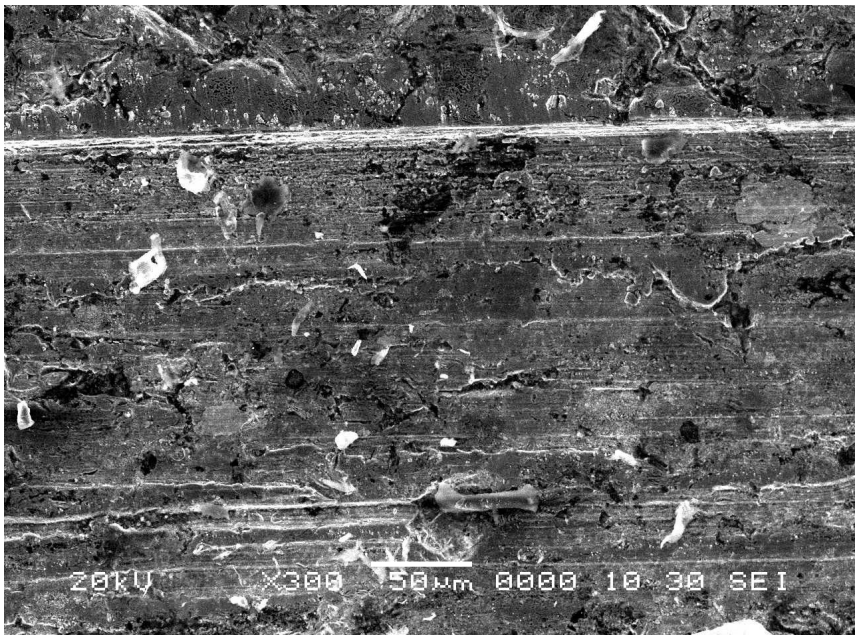

Fig. 5.15: Worn out surface of segment of gang saw (SGS) showing longitudinal cracks along the sliding direction
(Pressure = 0.4 MPa, sliding distance=3000m, sliding velocity = 2.4m/s))

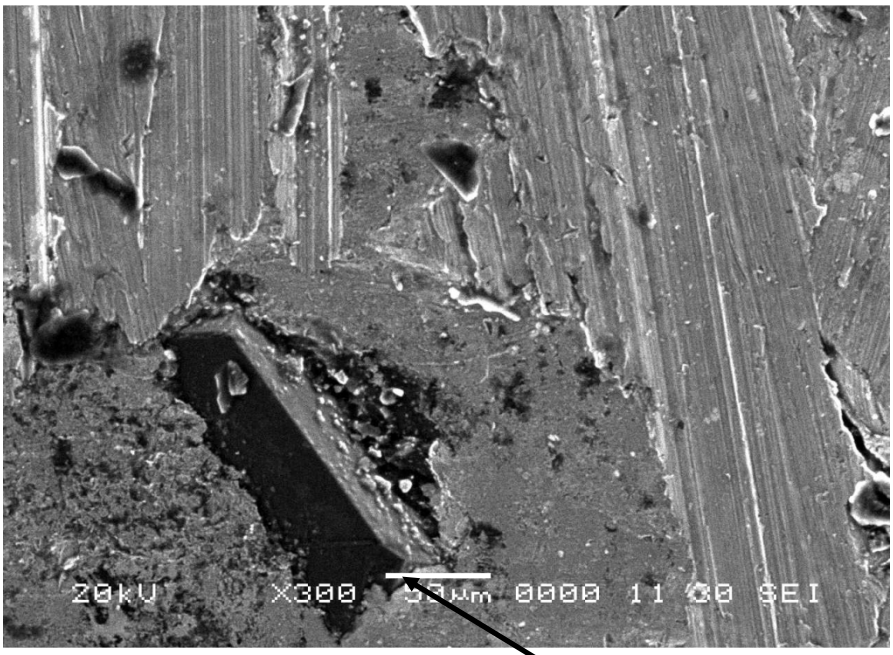

Diamond particle

Fig. 5.16: Worn out surface of DCT containing 9.37% Sn showing sharp cutting edge of Diamond exposed while sliding and indication of cracks due to severe deformation. (Pressure = 0.4 MPa, sliding distance=3000m, sliding velocity = 2.4m/s))

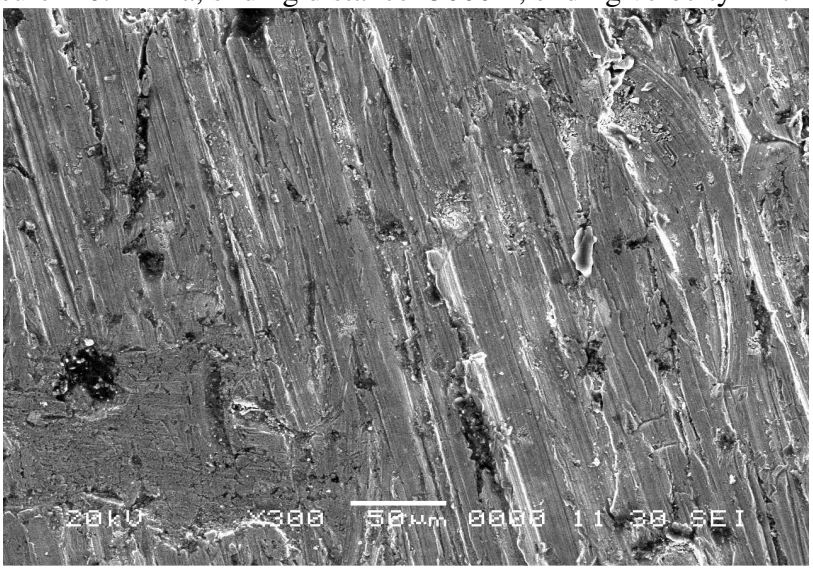

Fig. 5.17: Worn out surface of DCT containing 5% Sn showing cracks due to Severe deformation occurred during sliding. (Pressure = 0.4 MPa, sliding distance=3000m, sliding velocity = 2.1m/s))

5.6: General discussion

Initial metallurgical analysis of DCTs like segment of gang saw and pre-alloyed powders has given clue for arriving at optimal composition of the powder blend. In the existing DCTs which are available in the market primarily consists of imported powders made out of the co-precipitation method or carbonyl iron powder. These cutting tools are essentially impregnated in-situ by low melting alloy for e.g. Cu-Sn.

Based on the understanding obtained from the metallurgical investigations of DCTs, the new formulation of powder blend was proposed in the present work. It consists of electrolytic iron powder, cobalt powder and Cu-Sn powder with reinforcements of synthetic diamonds and tungsten carbides. It is observed that the infiltration of Cu or Cu-Sn alloy carried out by ex-situ process gave rise to limited level of improvements especially hardness and wear resistance but sintered density was appreciable. However tools fabricated by in-situ process showed sweating problem when tin content was 9.37%, but this was later brought down to 5% to avoid operational difficulties during processing. In order to make fabrication of DCTs techno-economically viable, it was necessary to carry out series of experiments to optimized Co content as well as the to reduce the sintering temperature. In the present work optimum Co content was found to be 8.52% and sintering temperature 810^0C in hot pressed conditions. The optimized chemical formulation of DCT was used to fabricate prototype tools at industrial level. The quality of these fabricated tools is meeting the desired criterion of the existing tools. The effect of WC to the level of from 2.88 to 5% and Co content from 8.52 to 15% was investigated on the fabricated DCTs and it has observed the negative effect on Wear properties and hardness for the same set of conditions.

CHAPTER 6
CONCLUSIONS

Based on results and discussions following conclusions can be drawn for developing Diamond Cutting Tools (DCTs),

1. Diamond cutting tools can be manufactured more effectively by using electrolytic iron powder instead of carbonyl iron powder.
2. In-situ sintering process gave better results than conventional ex-situ sintering process.
3. It is possible to fabricate DCTs with reduced amount of Co (8.52%.by wt).
4. Sintering temperature is reduced to 810^0C using 5% Sn, further increase amount of tin gives rise to sweating problem which might causes difficulties in fabrication.
5. Cutting tools fabricated by powder metallurgy route shows inherent heterogeneity in properties as evident from standard deviation.
6. Premixing of powders is found to be successful for making DCTs than pre-alloyed and co-precipitation methods.
7. Material cost saving by 20% is possible for manufacturing of prototype DCTs.

CHAPTER-7.

FUTURE SCOPE

Smaller diamond particles should give large cutting action But this is not in practice due to as it get dislodge during cutting operations hence bigger size around 90 as it get sufficiently embedded in the matrix. It is proposed to develop a systematic model to evaluate a critical size of the diamond particle.

It is necessary to evaluate wear mechanism for the diamond Cutting tools.

References:

[1] Janusz Konstanty., *Powder Metallurgy Diamond Tools*, 2005, pp 69- 72

[2] Randell M. German., *Powder metallurgy science*, 1994, second edition, 210-212 and 270-275

[3] ASM handbook , 2004,vol 3, pp 2.140-2.168

[4] Steven W. Webb, *Diamond retention in sintered cobalt bonds for stone cutting and drilling,* Diamond Related Material 8 (1999)2043-2052

[5]Sadi Karagoz, Muzaffer Zaren, *The property of diamond-cutting tools with the help of micro-structural characterization,* International Journal of Refractory Metals and Hard Materials 19 (2001)23-26

[6] H.K.Tonshoff, H.Hillmann-Apmann, J. Asche, *Diamond tools in stone and civil engineering industry: cutting principles, wear and applicatons*, Diamond and Related Materials 11 (2002)736-741.

[7] C.Y.Wang, R.Clausen *, Marble cutting with single point cutting tool and diamond segments,* International Journal of Machine Tools and Manufacture 42 (2002) 1045-1054.

[8] Luciano Jose de Oliveira, Guerlold Sergueevitch Bobrovintichii, Marcello Filgueira, *Processesing and characterization of impreganted diamond cutting tools using a ferrous metal matrix*, International Journal of refractory metals and hard materials 25(2007)328-335

9] Z. Nitkiewicz, M.Swierzy, *Tin influence on cutting behavior of diamond saw blades for stone cutting,* 13th International scientific Conference on Achievements in Mechanical and Material Engineering ,16th-19th May 2005,Polond.

10]Alegandro Ordonez Torres, Roberto Gonzalez Ojeda, *Characterization of Diamond Particles in Stone-Cutting tools Applications.*

11] S.Silva, V.P.Mammana,,M.C.Salvadori,O.R.Monterio,I.G.Brown, *WC-Co cutting Tool Inserts with Diamond Coatings,* Diamond and Related Materials 8 (1999) 1913-1918.

12] R.R. Thorat, P.K.Brahmankar, T.R.R.Mohan, *Consolidation Behavior of Cu-Co-Fe Prealloyed Powders* ,International Symposium of Research students on Materials Science and Engineering, Dec20-22,2004,Chennai,India.

13] y.Sakka, T. Uchikoshi, E.Ozawa, *Sintering characteristics of Fe and FeCo alloy ultrafine powders*, Journal of Materials Science 28,(1993) 203-217.

14] W. Telmann, C. Kronholz, M. Ferreira, *Comparison of different metal matrix systems for dimond tools fabricated by new current short-time sintering processes,* PM 2010 World Congress- Diamond Tools.

APPENDICES

Appendix 1: EDS reports

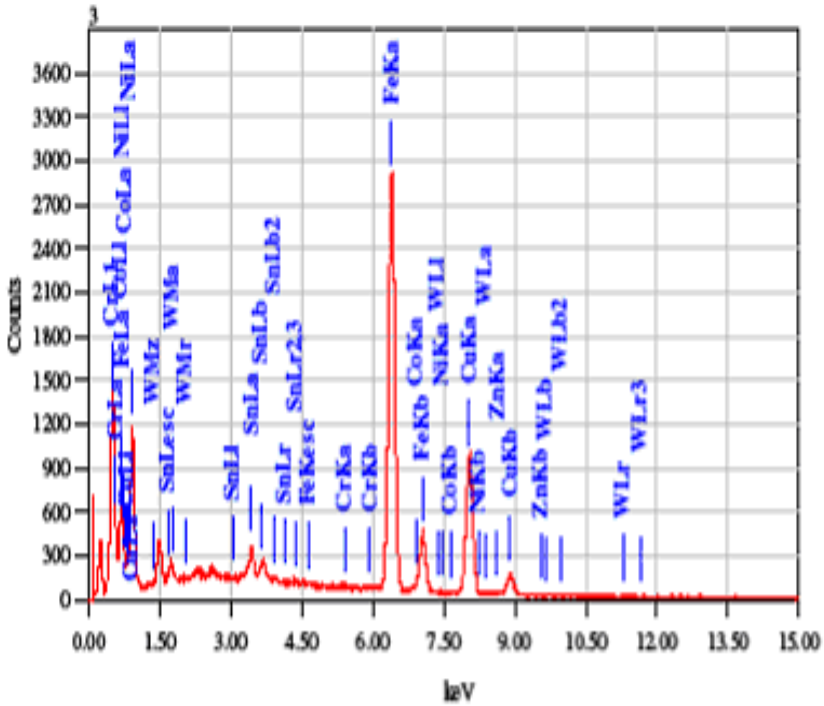

Acquisition Parameter
Instrument : 6360(LA)
Acc. Voltage : 20.0 kV
Probe Current: 1.00000 nA
PHA mode : T3
Real Time : 75.44 sec
Live Time : 50.00 sec
Dead Time : 33 %
Counting Rate: 8155 cps
Energy Range : 0 - 20 keV

ZAF Method Standardless Quantitative Analysis
Fitting Coefficient : 0.3199

Element	(keV)	mass%	Error%	At%	Compound	mass%	Cation	K
Cr K	5.411	0.11	0.32	0.13				0.1230
Fe K	6.398	56.03	0.41	60.61				58.9961
Co K								
Ni K	7.471	0.02	0.70	0.02				0.0203
Cu K	8.040	37.75	0.91	35.89				35.2953
Zn K	8.630	0.98	1.13	0.90				0.9270
Sn L	3.442	4.29	0.52	2.19				3.6850
W M	1.774	0.82	0.85	0.27				0.4136
Total		100.00		100.00				

Fig:1 EDS report for SGS

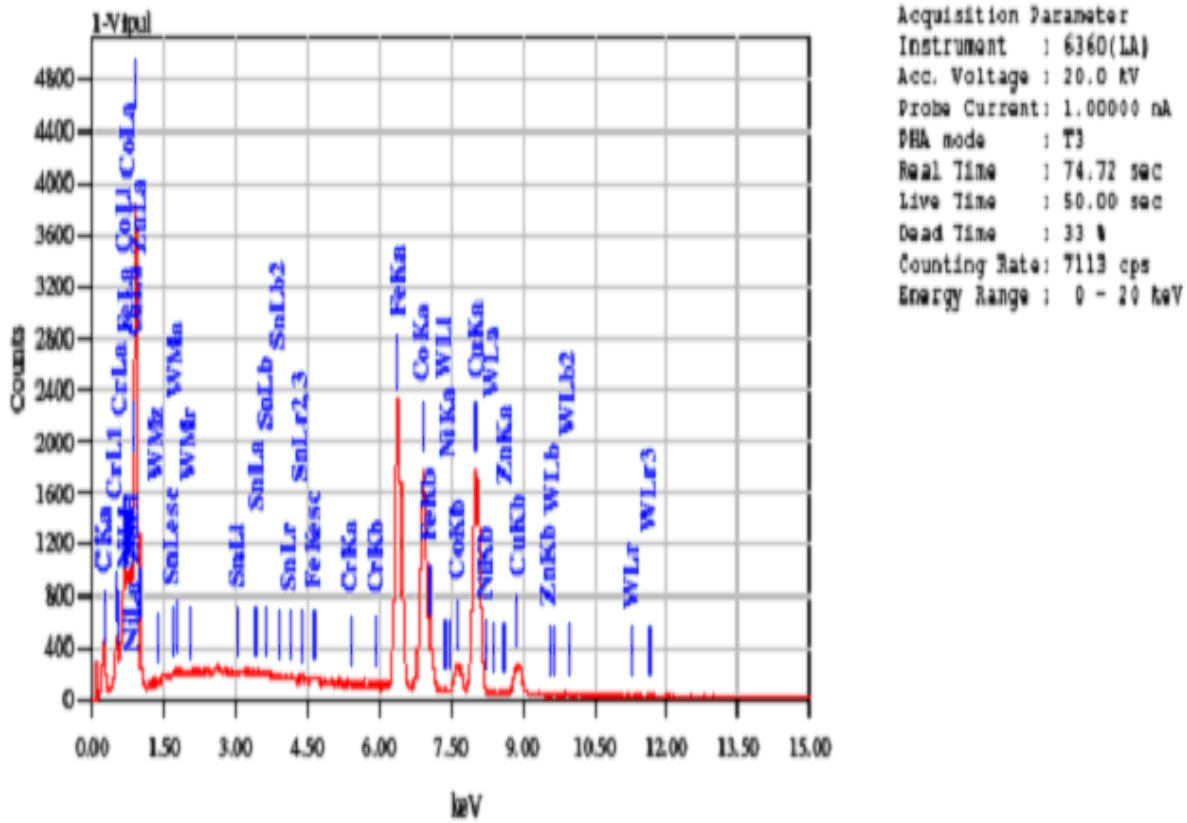

ZAF Method Standardless Quantitative Analysis
Fitting Coefficient : 0.1926

Element	(keV)	mass%	Error%	At%	Compound	mass%	Cation	X
C K	0.277	11.12	0.14	38.48				2.2700
Cr K	5.411	0.14	0.11	0.11				0.1653
Fe K	6.398	25.99	0.15	19.34				30.0039
Co K	6.924	22.26	0.18	15.70				25.8233
Ni K								
Cu K	8.040	39.93	0.32	26.12				40.5897
Zn K	8.630	0.30	0.40	0.19				0.3051
Sn L	3.442	0.04	0.19	0.01				0.0398
W M	1.774	0.24	0.30	0.05				0.1311
Total		100.00		100.00				

Fig: 2 EDX report for sample A

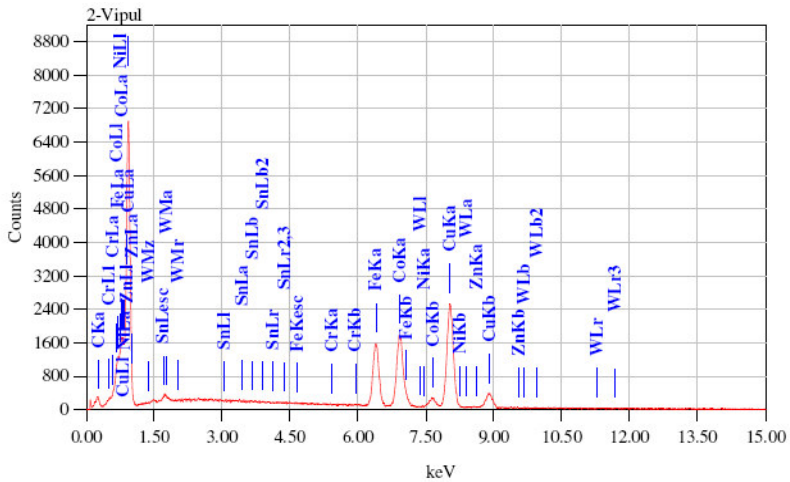


```
Acquisition Parameter
Instrument    : 6360(LA)
Acc. Voltage  : 20.0 kV
Probe Current: 1.00000 nA
PHA mode      : T3
Real Time     : 78.41 sec
Live Time     : 50.00 sec
Dead Time     : 37 %
Counting Rate: 8399 cps
Energy Range :  0 - 20 keV
```

ZAF Method Standardless Quantitative Analysis
Fitting Coefficient : 0.1344

Element	(keV)	mass%	Error%	At%	Compound	mass%	Cation	K
C K	0.277	5.99	0.12	24.48				1.1011
Cr K	5.411	0.04	0.09	0.03				0.0410
Fe K	6.398	16.04	0.11	14.10				18.0723
Co K	6.924	21.92	0.14	18.27				25.1205
Ni K	7.471	0.17	0.19	0.14				0.1837
Cu K	8.040	55.15	0.25	42.63				54.4553
Zn K	8.630	0.33	0.31	0.24				0.3252
Sn L								
W M	1.774	0.36	0.25	0.10				0.1824
Total		100.00		100.00				

Fig.3: EDS report for sample A

Appendix 2 : Results for individual powders

Table 4.7: Details of process parameters and results obtained during individual powder analysis

Type of Powder	Compacting Pressure (MPa)	Sintered at 870^{0}C		Sintered at 920^{0}C	
		Density (g/cc)	Hardness (HRB)	Density (g/cc)	Hardness (HRB)
Cu	400	8.0034	64.3	8.36	90.3
	450	8.0736	76.8	8.42	93.8
	500	8.2478	88.3	8.431	79.3
	550	8.245	87.3	8.489	68.3
Fe	400	6.657	22.8	6.498	22.3
	450	6.795	27.3	6.74	20.8
	500	6.862	36.8	6.815	30.3
	550	6.924	38.8	7.09	26.3
Co	400	8.5149	94.8	8.481	95.3
	450	8.5157	92.3	8.531	95.8
	500	8.595	92.3	8.58	96.8
	550	8.589	92.3	8.505	97.8

Appendix 3: Results for optimization of sintering parameters for Expt No.4 and 5

Table 4.9: Showing values of density, hardness and wear rate at different sintering time.

Sintering time	15 min	30 min	45 min	60 min
Sintered density (g/cc)	7.6	**8.295**	7.54	7.64
Hardness (HRB)	64.8	**73.63**	57.133	53.3
Wear Rate (mm^3/m)	0.00395	**0.00317**	0.0032	0.00357

Table 4.10: Showing values of density, hardness and wear rate at different sintering temperatures

	Ts = 870^0C	Ts = 950^0C
Sintered Density (g/CC)	**8.295**	7.29
Hardness (HRB)	**73.63**	46.3
Wear Rate (mm^3/m)	**0.00317**	0.003199